



Review of physics-informed neural networks in hemodynamics[☆]

Xianglong Yu ^a, Yu Hu ^a, Rui Guo ^b, Lei Fan ^c, Haiyan Ding ^d, Jingjing Xiao ^a,*

^a Bio-Med Informatics Research Center, The Second Affiliated Hospital, Army Medical University, Chongqing, 400037, China

^b School of Medical Technology, Beijing Institute of Technology, Beijing, 100081, China

^c Department of Civil Engineering, Xi'an Jiaotong-Liverpool University, Suzhou, 215123, China

^d Center for Biomedical Imaging Research, School of Biomedical Engineering, Tsinghua University, Beijing, 100084, China



ARTICLE INFO

Keywords:

Physics-informed neural networks

Hemodynamics

Cardiovascular flow

Medical image-based simulation

ABSTRACT

The circulatory system sustains physiological function through oxygen transport, nutrient delivery, and waste clearance, all of which rely on efficient blood flow. Accurate characterization and quantification of hemodynamics are essential for the diagnosis and treatment of cardiovascular diseases. However, assessing blood flow in a noninvasive and real-time manner remains a major challenge, as current imaging modalities often suffer from limited spatial and temporal resolution, while traditional computational fluid dynamics algorithms are computationally intensive and sensitive to anatomical and physiological uncertainties. Physics-informed neural networks (PINNs), combining physical laws with data-driven learning, provide a promising framework to connect computational modeling with clinical applications. In this review, we provide a comprehensive overview of recent advances in the application of PINNs to hemodynamics. We introduce theoretical foundations, highlight methodological innovations, and discuss applications in simulating blood flow under physiological and pathological conditions, as well as in estimating clinically relevant hemodynamic parameters. Importantly, our analysis highlights that PINNs achieve comparable accuracy to traditional methods while unlocking novel opportunities for patient-specific diagnosis and risk prediction. We conclude with a discussion of the benefits, current limitations, and future directions of PINNs in cardiovascular research, underscoring the transformative potential to accelerate clinical translation through interdisciplinary collaboration.

1. Introduction

Cardiovascular disease (CVD) remains the leading cause of morbidity and mortality worldwide, posing a significant burden on public health and healthcare systems (Kazi et al., 2024; Li et al., 2025). Clinical studies have consistently found that diseases such as atherosclerosis, myocardial infarction, and stroke are closely coupled to abnormalities in blood flow dynamics (Gijzen et al., 2019; Chen et al., 2024), emphasizing the critical role of hemodynamics in onset, progression, and prognosis of CVD. Consequently, accurate characterization of hemodynamic behavior in circulatory system is essential for early diagnosis, risk assessment, treatment planning, and therapeutic monitoring.

Despite its clinical importance, direct and continuous *in vivo* measurement of hemodynamics remains challenging due to the complex geometry of vascular networks, the invasiveness nature of catheter- or pressure-wire-based measurement, and the associated medical costs. In this context, biomedical imaging modalities, such as ultrasound (US), magnetic resonance imaging (MRI) (Si et al., 2023; Guo et al., 2022),

computed tomography (CT), and optical coherence tomography (OCT), have enabled the noninvasive visualization of vascular structures and blood flow. For instance, Doppler ultrasound technology provides real-time assessments of flow velocity and direction based on frequency shifts, but is inherently limited to one-dimensional (1D) measurements along the beam axis (Suriani et al., 2022).

Complementary to imaging, computational fluid dynamics (CFD) has emerged as a powerful approach for simulating blood flow based on anatomical imaging data and mathematical models of fluid motion, such as the Navier-Stokes equations (Philip et al., 2022). CFD enables detailed, patient-specific analysis of vascular hemodynamics by integrating imaging-derived geometries and physiologically relevant boundary conditions, thereby providing insights into flow patterns, pressure gradients, and wall shear stresses (WSS). Conventional CFD techniques, as well as finite element methods (FEM) and finite difference methods, have shown high fidelity but remain computationally demanding and sensitive to assumptions on boundary conditions (Wang

[☆] This article is part of a Special issue entitled: 'PIML in Engineering Applications' published in Engineering Applications of Artificial Intelligence.

* Corresponding author.

E-mail address: shine636363@sina.com (J. Xiao).

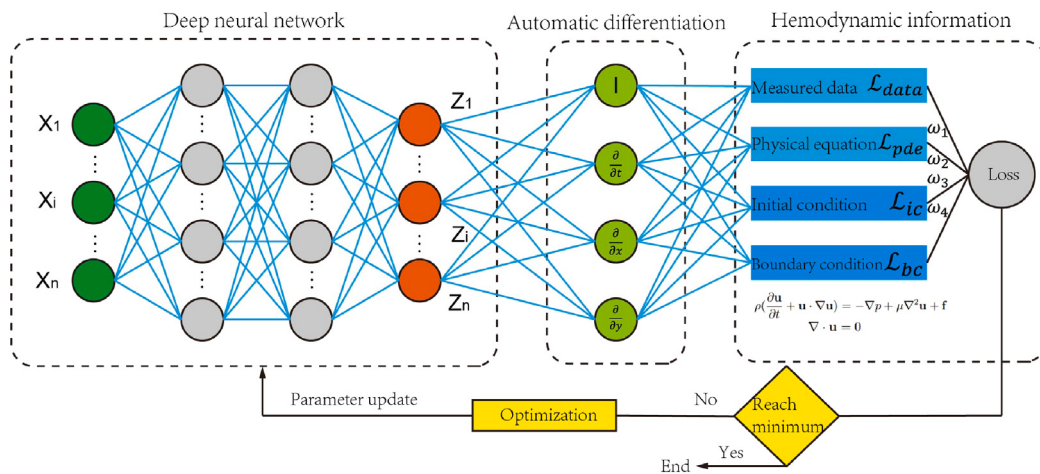


Fig. 1. Framework of PINNs for solving general computational hemodynamics problems. The deep neural network receives spatial and temporal inputs (\mathbf{x}, t) and generates outputs such as velocity \mathbf{u} and pressure p , which are differentiated using automatic differentiation to evaluate physical constraints. The loss function combines contributions from measured data, governing equations, and initial and boundary conditions. Through iterative optimization, the network parameters are updated until convergence, enabling accurate blood flow simulation consistent with hemodynamic laws.

et al., 2022). Moreover, CFD integration into clinical workflows is hindered by the need for domain-specific expertise and lengthy simulation times (Sadeghi et al., 2022).

Recent advances in machine learning (ML) have shown promise in augmenting biomedical image analysis and predictive modeling in cardiovascular applications. Deep learning approaches have been employed to estimate hemodynamic parameters, such as fractional flow reserve (FFR) derived from CT, flow velocity, pressure distribution (Liu et al., 2021; Berhane et al., 2020). Nevertheless, purely data-driven models often suffer from limited resolution, poor generalizability, and a lack of physical interpretability, which are crucial for reliable biomedical applications, especially in hemodynamics where physical laws govern system behavior.

To bridge the gap between data-driven approaches and physics-based modeling, physics-informed neural networks (PINNs) (Raissi et al., 2019) have been proposed as a hybrid framework that embeds physical laws in the form of partial differential equations (PDEs) into the training of neural networks. Unlike classical numerical methods, PINNs leverage automatic differentiation to evaluate differential operators in the loss function or governing equations, eliminating numerical truncation errors and mitigating the curse of dimensionality. Furthermore, compared with purely data-driven algorithms, PINNs explicitly encode underlying physical principles, which enhances generalizability across diverse settings and improves model interpretability.

In the context of hemodynamics, PINNs have demonstrated promise by unifying two fundamental classes of problems: forward problems, where flow and pressure fields are simulated under prescribed boundary conditions, and inverse problems, where unknown parameters such as boundary conditions, material properties, or latent hemodynamic states are inferred from limited or noisy observations. This dual capability allows PINNs not only to simulate blood flow in physiological and pathological conditions (Raissi et al., 2020; Karniadakis et al., 2021), including aneurysms, stenosis, and atherosclerosis, but also to estimate clinically critical parameters such as WSS, pressure gradients, and flow rates. Therefore, PINNs provide a powerful framework to bridge patient-specific data with mechanistic models, thereby supporting more precise diagnosis, risk stratification, and personalized treatment planning in cardiovascular medicine.

Given the growing interest and rapid progress in this field, a timely review focused on the applications of PINNs in hemodynamics is warranted. While most existing reviews have addressed PINNs applications in fluid mechanics (Cai et al., 2021b), solid mechanics (Hu et al.,

2024), and broader engineering fields (Farrag et al., 2025), this work aims to fill a critical gap by offering a focused and comprehensive overview of PINNs in cardiovascular flow analysis. We begin by introducing the theoretical foundations and methodological innovations of PINNs. Next, we discuss the applications in simulating blood flow under both physiological and pathological conditions as well as the use in inverse modeling and parameter estimation. Finally, we conclude with an evaluation of current limitations, clinical relevance, and future directions.

2. Framework of PINNs

This section presents a detailed overview of the foundational principles of the PINNs, starting from the governing equations and culminating in the final training process. In addition, the latest advancements in PINNs methodologies are briefly summarized.

2.1. Fundamental concepts of PINNs

Hemodynamic phenomena, such as blood flow in large or medium-sized vessels, are typically governed by the incompressible Navier–Stokes equations (Mustafa Turkyilmazoglu, 2025; Larson and Wei, 2019) in the form of

$$\rho \left(\frac{\partial \mathbf{u}}{\partial t} + \mathbf{u} \cdot \nabla \mathbf{u} \right) = -\nabla p + \mu \nabla^2 \mathbf{u} + \mathbf{f}, \quad (\mathbf{x}, t) \in \Omega \times [0, T] \quad (1)$$

$$\nabla \cdot \mathbf{u} = 0, \quad (\mathbf{x}, t) \in \Omega \times [0, T] \quad (2)$$

where $\mathbf{x} = [x, y, z]$ and t denote the spatial coordinates and time, ρ is the blood density, μ is the dynamic viscosity, \mathbf{f} is the external force per unit volume, $\Omega \in \mathbb{R}^3$ is the fluid domain, and the primary variables to be solved are the velocity field $\mathbf{u} = [u, v, w]$ and pressure p subject to appropriate initial and boundary conditions

$$\mathcal{I}(\mathbf{x}, \mathbf{u}, p) = 0, \quad \mathbf{x} \in \Omega, t = 0 \quad (3)$$

$$\mathcal{B}(\mathbf{x}, t, \mathbf{u}, p) = 0, \quad (\mathbf{x}, t) \in \partial\Omega \times [0, T] \quad (4)$$

where \mathcal{I} and \mathcal{B} denote the differential operators that specify the initial and boundary conditions, respectively. These conditions may include both Dirichlet and Neumann boundary conditions depending on the specific hemodynamic scenario.

PINNs represent a novel paradigm that seamlessly integrates deep learning with physical modeling, enabling efficient and accurate solutions to PDEs across spatiotemporal domains. As illustrated in Fig. 1, a

fully connected feedforward neural network (FNN), denoted as $\mathcal{N}(\mathbf{x}, t)$, approximates the solution of the governing equations by mapping input coordinates (\mathbf{x}, t) to outputs such as velocity \mathbf{u} and pressure p .

The architecture of the network is defined recursively as follows

$$\mathcal{N}^0(\mathbf{x}, t) = \mathbf{x} \in \mathbb{R}^{d_{\text{in}}} \quad (5)$$

$$\mathcal{N}^l(\mathbf{x}, t) = \sigma(\mathbf{W}^l \mathcal{N}^{l-1}(\mathbf{x}, t) + \mathbf{b}^l) \in \mathbb{R}^{N_l} \quad \text{for } 1 \leq l \leq L - 1 \quad (6)$$

$$\mathcal{N}^L(\mathbf{x}, t) = \mathbf{W}^L \mathcal{N}^{L-1}(\mathbf{x}, t) + \mathbf{b}^L \in \mathbb{R}^{d_{\text{out}}} \quad (7)$$

where l and L denote the current hidden layer index and the total number of layers, respectively; \mathbf{W}^l and \mathbf{b}^l represent a weight matrix and bias vector in the l -th layer, and $\sigma(\cdot)$ indicates the activation function. The input variables are spatial and time coordinates (\mathbf{x}, t) , while the output variables typically include the velocity field \mathbf{u} and pressure p .

A key innovation of PINNs lies in the embedding of governing physical laws, typically in the form of PDEs, directly into the loss function of the neural network. This allows the network to respect both data fidelity and physical consistency. To this end, the total loss function \mathcal{L} is a weighted summation of data-driven term $\mathcal{L}_{\text{data}}$ and a set of physical consistent loss term \mathcal{L}_{phy} , which includes physical equation loss term \mathcal{L}_{pde} , initial condition loss term \mathcal{L}_{ic} , and boundary condition loss term \mathcal{L}_{bc}

$$\mathcal{L} = \underbrace{w_1 \mathcal{L}_{\text{data}}}_{\text{data-driven loss}} + \underbrace{w_2 \mathcal{L}_{\text{pde}} + w_3 \mathcal{L}_{\text{ic}} + w_4 \mathcal{L}_{\text{bc}}}_{\text{physics consistent losses}} \quad (8)$$

where $[w_1, w_2, w_3, w_4]$ are the weighting coefficients for different loss terms. The sub-losses are defined as follows:

$$\mathcal{L}_{\text{data}} = \|\mathcal{N}_u - \mathbf{u}_{\text{obs}}\| + \|\mathcal{N}_p - p_{\text{obs}}\| \quad (9)$$

$$\mathcal{L}_{\text{pde}} = \|\rho \left(\frac{\partial \mathcal{N}_u}{\partial t} + \mathcal{N}_u \cdot \nabla \mathcal{N}_u \right) + \nabla \mathcal{N}_p - \mu \nabla^2 \mathcal{N}_u - \mathbf{f}\| + \|\nabla \cdot \mathcal{N}_u\| = 0 \quad (10)$$

$$\mathcal{L}_{\text{ic}} = \|\mathcal{N}_u(\mathbf{x}, t=0) - \mathcal{I}(\mathbf{x}, \mathbf{u}, p)\|, \quad \mathbf{x} \in \Omega, t=0 \quad (11)$$

$$\mathcal{L}_{\text{bc}} = \|\mathcal{N}_u(\mathbf{x}, t) - \mathcal{B}(\mathbf{x}, t, \mathbf{u}, p)\|, \quad (\mathbf{x}, t) \in \partial\Omega \times [0, T] \quad (12)$$

where $\|\cdot\|$ is the L_2 error norm, \mathcal{N}_u and \mathcal{N}_p represent the network output velocity and pressure, \mathbf{u}_{obs} and p_{obs} are the observed or measured velocity and pressure data, respectively.

Consequently, solving the blood flow equations is formulated as an optimization problem with the goal to minimize the loss function by iteratively update network parameters until convergence is achieved below a predefined tolerance

$$\theta^* = \arg \min_{\theta} \mathcal{L} \quad \text{s.t.} \quad \begin{cases} \mathcal{I}(\mathbf{x}, \mathbf{u}, p) = 0, & \mathbf{x} \in \Omega, t=0 \\ \mathcal{B}(\mathbf{x}, t, \mathbf{u}, p) = 0, & (\mathbf{x}, t) \in \partial\Omega \times [0, T] \end{cases} \quad (13)$$

where $\theta = [\mathbf{W}, \mathbf{b}]$ denotes the set of trainable network parameters, including weights and biases.

It should be noted that convergence alone does not guarantee that the solution is physically consistent. To mitigate bias and ensure that the converged solution remains faithful to the underlying hemodynamic laws, several strategies are typically employed: (1) applying appropriate normalization and weighting of different loss terms to balance data fidelity with physical consistency; (2) validating PINN predictions against analytical benchmarks, high-fidelity simulations, or experimental or clinical measurements; and (3) employing adaptive sampling strategies to focus training on regions of high error or physical significance. These practices collectively enhance the reliability of PINNs in producing physically plausible hemodynamic solutions.

In summary, PINNs serve as an unsupervised learning method in forward problems where no observational data are available, relying solely on governing equations and boundary conditions. Moreover, in inverse problems particularly when estimating parameters from noisy or partial observations, PINNs act as a supervised or semi-supervised learning framework, offering robust generalization and physical consistency.

2.2. Recent methodological advancements of PINNs

Based on the foundational formulations of PINNs, a wide range of methodological innovations have been introduced to overcome inherent limitations and improve model performance. As shown in Fig. 2, recent methodological progress encompasses several critical aspects, including network architecture, loss function design, activation functions, optimization algorithms, differentiation algorithms, and sampling strategies. Together, these developments have significantly enhanced the capacity of PINNs to tackle complex problems in physics and engineering domains, particularly in hemodynamics.

Traditional PINNs rely on FNNs with multilayer perceptron (MLP) structures. However, these architectures often struggle to capture multi-scale features, especially in high-gradient regions or geometrically complex domains. To address this, alternative architectures such as convolutional neural networks (CNN) (Gao et al., 2021; Pashaei Kalajahi et al., 2025), Fourier Neural Operators (FNOs) (Thodi et al., 2024), and Deep Operator Networks (DeepONets) (Lu et al., 2021a; Wang et al., 2021) as shown in Fig. 2(a) have been proposed. These operator-based models improve generalizability by learning solution operators instead of point-wise mappings. Empirical studies also show that network depth and width critically affect solution accuracy, though no universally optimal architecture has yet been established for real-world hemodynamic problems.

Standard formulations of loss function in PINNs employ a weighted sum of data-driven loss and physics-informed loss, while manual weight tuning leads to slow convergence and instability. To mitigate this, adaptive weighting strategies (McClenny and Braga-Neto, 2023; Li et al., 2022) introduce learnable scaling factors ϵ to dynamically balance loss terms during training, as depicted in Fig. 2(b). Alternative formulations, such as the incorporation of Lagrange multipliers (Lu et al., 2021b), enforce boundary conditions as hard constraints. Variational PINNs (Kharazmi et al., 2021) which are derived from variational principles improve numerical stability and accuracy. Energy-based losses (Samaniego et al., 2020; Yu and Zhou, 2023) have also proven effective in fluid and solid mechanics by reducing the order of governing equations.

Traditional activation functions in PINNs like ReLU and tanh exhibit spectral bias, making it difficult to capture high-frequency components in blood flow simulations. To overcome this, adaptive activation functions (Jagtap et al., 2020) presented in Fig. 2(c) are developed where the scaling factor a is learnable during training. Additionally, composite activation strategies, where multiple activation functions are used in different network layers, have been proposed to further enhance the performance of PINNs (Zafar et al., 2025).

Training PINNs is challenging due to the highly non-convex nature of the loss landscape. Common optimizers like Adam (first order) and L-BFGS (quasi second order) suffer from slow convergence and entrapment in local minima when applied to stiff PDEs, as shown in Fig. 2(d). Second-order optimization methods such as quasi-Newton approaches (Heger et al., 2024), have also been investigated to improve convergence in high-resolution simulations. Additionally, networks are initially trained on simplified problems or synthetic data can lead to faster and more stable convergence when transferred to real-world applications (Zhou and Yu, 2024).

As the core feature of PINNs, automatic differentiation provides machine-precision gradients by leveraging the computational graph. However, automatic differentiation can become ineffective when collocation points are sparse or located near discontinuities (Yu and Zhou, 2024a,b). In contrast, numerical differentiation remains robust and accurate in such contexts (Yuan et al., 2022). To exploit the strengths of both, hybrid differentiation schemes have been proposed (Chiu et al., 2022), combining the flexibility of automatic differentiation with the stability of numerical differentiation, as shown in Fig. 2(e).

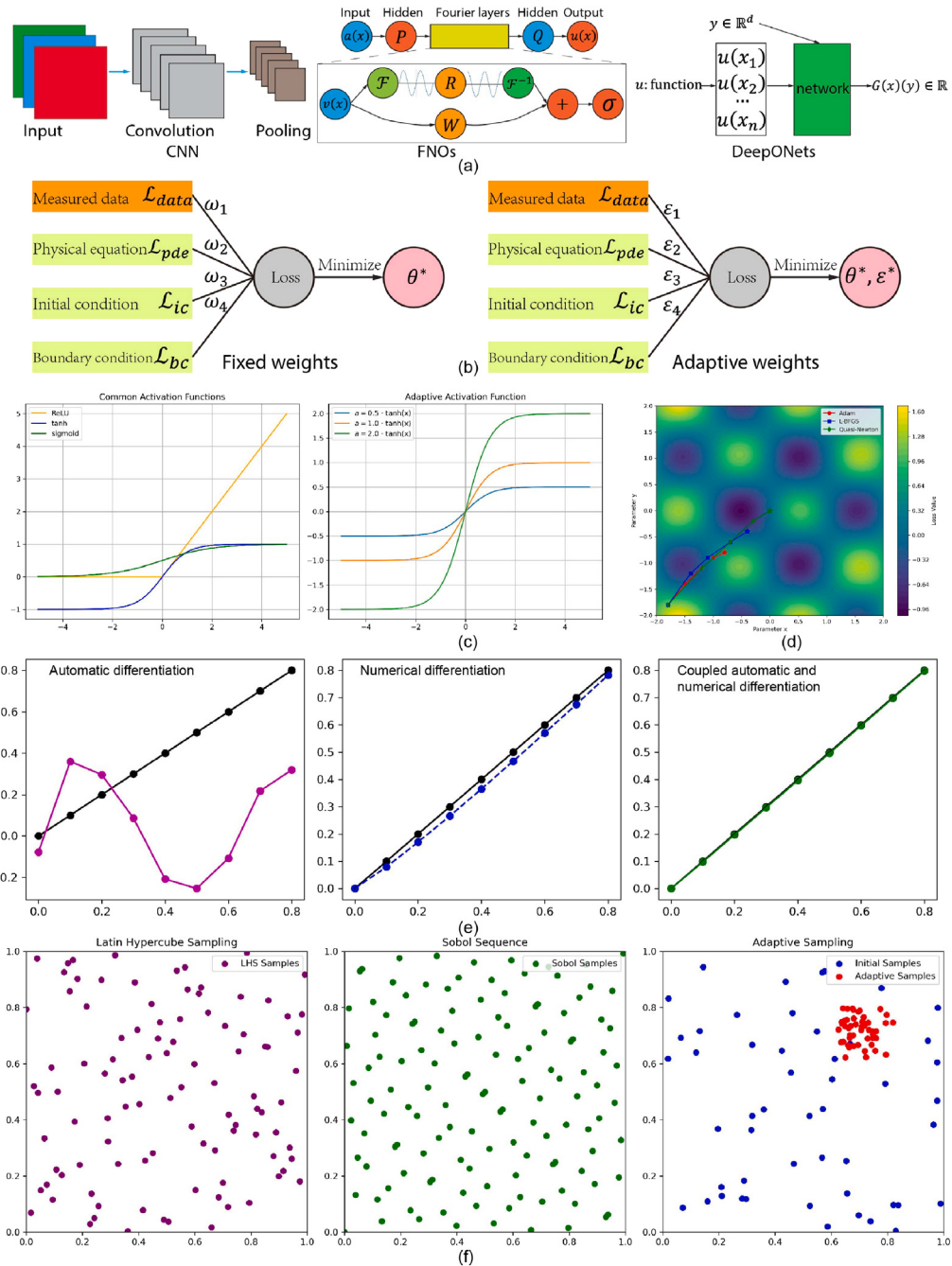


Fig. 2. Recent advancements in PINNs across key technical domains: (a) Novel architectures such as CNN, FNOs, and DeepONets expand model capacity. (b) Loss function design can use fixed or adaptive weights to balance contributions from data, governing equations, and boundary conditions. (c) Adaptive activation functions improve convergence and flexibility. (d) Advanced optimization algorithms guide training in high-dimensional parameter spaces. (e) Differentiation strategies include automatic, numerical, or hybrid approaches for evaluating physical residuals. (f) Sampling strategies such as Latin hypercube, Sobol, and adaptive sampling improve training efficiency.

Finally, sampling strategies play a crucial role in the efficiency and accuracy of PINNs training. Conventional PINNs use non-adaptive sampling (e.g., Random, Latin hypercube or Sobol sequences) in Fig. 2(f) to generate collocation points, which may poorly resolve local phenomena such as boundary layers or flow separation zones. To address this, adaptive sampling techniques have been developed to dynamically add collocation points in regions with high PDE residuals (Wu et al., 2023), thereby improving accuracy and reducing redundancy. Additionally,

prioritize sampling in critical regions (Raissi et al., 2020) (e.g., vessel bifurcations, stenotic regions) have been shown to significantly enhance PINNs performance in blood flow modeling.

3. Applications of PINNs in hemodynamics

PINNs have shown significant promise in the field of hemodynamics, with a growing number of publications reflecting their increasing adoption. The bibliographic network illustrated in Fig. 3, collected

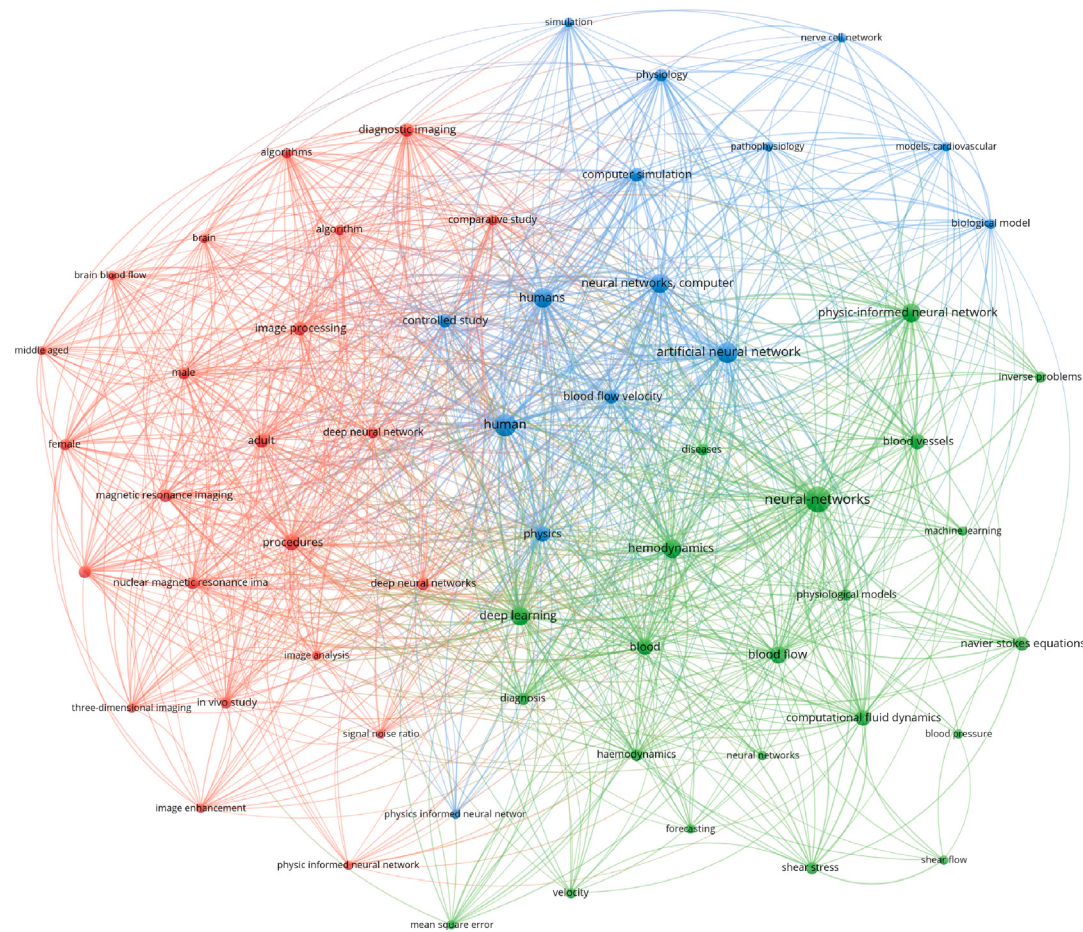


Fig. 3. Bibliographic analysis of literature associated with PINNs in hemodynamics. The network map illustrates the co-occurrence of keywords in published studies, with node size representing frequency and edge thickness indicating strength of co-citation. Three major clusters are visible: (1) imaging and diagnostic applications (red), (2) clinical and physiological terms (blue), and (3) CFD and modeling concepts (green). This analysis highlights the interdisciplinary nature of PINNs-based hemodynamic research, bridging medical imaging, computational modeling, and clinical practice.

Table 1
Categorized applications of PINNs in hemodynamics.

Application domain	Characteristics	References
General blood flow	3D Navier–Stokes equation	Zhang and Tai (2024), Gu et al. (2024), Liu et al. (2024) and Williams et al. (2023)
	1D Navier–Stokes equation	Li et al. (2024), Changdar et al. (2024), Dobroserdova et al. (2024), Bhaumik et al. (2024), Zhang et al. (2024b) and Chang et al. (2024)
Anatomical-specific	Stenosis and aneurysm	Arzani et al. (2021), Zhang et al. (2024a), Cai et al. (2021a), Liu et al. (2025), Moser et al. (2023), Wang et al. (2025), Sautory and Shadden (2024) and Shi et al. (2024)
	Aorta hemodynamics	Liang et al. (2023), Aghaee and Khan (2024, 2025), Sen et al. (2024), Zhang et al. (2023), Kang et al. (2024), Ur Rehman et al. (2025) and Kissas et al. (2020)
	Cardiac hemodynamics	Oldenburg et al. (2022), Buoso et al. (2021), Wong et al. (2025), Maidu et al. (2025), Naghavi et al. (2024), Ling et al. (2024), Alzhanov et al. (2024b) and Alzhanov et al. (2024a)
	Cerebral hemodynamics	Galazis et al. (2025), Rotkopp et al. (2024), Voorter et al. (2023), Wang et al. (2024), Sarabian et al. (2022), Voorter et al. (2025), Ferdian et al. (2023) and Ishida et al. (2024a)
Parameter estimation	Vascular hemodynamics estimation	Garay et al. (2024), Isaev et al. (2024), Du et al. (2023) and Boster et al. (2023)
	Medical imaging-based quantification	Ishida et al. (2024b), van Herten et al. (2022), Ferrante et al. (2024) and Liang et al. (2025)
	Physiological and multiscale systems	Qian et al. (2024), Sel et al. (2023), Oszkinat et al. (2023) and Sotero et al. (2024)

by searching specific keywords such as “physics-informed neural networks”, “physics-informed”, “hemodynamics” and “blood flow” in SCOPUS and Web of Science databases, illustrates the breadth and interdisciplinary nature of the field. The analysis reveals distinct clusters linking computational modeling, medical imaging, and clinical applications, underscoring how PINNs-based approaches are increasingly positioned at the intersection of engineering and healthcare.

These applications cover a wide range of hemodynamic contexts, as summarized in Table 1, including general blood flow simulation,

as well as domain-specific analyses involving the aorta, heart, and cerebral vasculature. Moreover, PINNs have been effectively applied to pathological conditions such as stenosis and aneurysms, covering both physiologically normal and severely altered flow states. In addition to forward simulations, PINNs are increasingly used to solve inverse problems, such as parameter estimation and boundary condition inference, based on sparse or noisy clinical data. This includes the reconstruction of velocity, pressure, and WSS fields from imaging data, as well as integration into physiological and multiscale modeling systems.

Table 2
Performance of PINNs models in blood flow analysis.

Problem	Reference method	Accuracy	Computational time
Blood flow simulation (Zhang and Tai, 2024)	FEM	ω :RE = 0.0441, p :RE = 0.0604	1711 s/2498 s
Vessel with plaque (Zhang et al., 2024a)	FEM	ω :RE = 0.0092, p :RE = 0.0173	9417 s
Microfluidic flow (Cai et al., 2021a)	CFD	ω : L_2 = ~ 10%	N/A
Flow in aneurysm (Liu et al., 2025)	FEM	ω : L_2 = 8.22e-02, p : L_2 = 3.84e-02, WSS: L_2 = 9.81e-01 ω :RMSE = 0.0002	63 h 53 min 35 s
Aorta wall deformation (Liang et al., 2023)	FEM		N/A
Patient-specific aorta (Aghaee and Khan, 2024)	CFD	ω :RAE = 15%-30%	N/A
Aorta with stenosis (Aghaee and Khan, 2025)	CFD	ω :RAE = 10%-20%	N/A
Carotid bifurcation (Sen et al., 2024)	In vivo data	ω : R^2 = 0.89-0.94	N/A
Aorta hemodynamics prediction (Zhang et al., 2023)	CFD	FFRct: R^2 = 0.9608, WSS: R^2 = 0.9813	1 s/43 200 s
Flow field reconstruction in left ventricle (Wong et al., 2025)	CFD	ω :RMSE = 4.96% ± 1.48%, v :RMSE = 1.98% ± 0.40%, w :RMSE = 4.65% ± 1.61%, p :RE = 0.70% ± 0.41%	1.8-4.48 days
Intraventricular vector flow mapping (Maidu et al., 2025)	Echocardiography	ω : R^2 = 0.84	15 min
Left ventricular contractility estimation (Naghavi et al., 2024)	CFD	RMAE < 2%	96 h/1000 h
Coronary artery tree FFR (Alzhanov et al., 2024b)	Invasive FFR	FFR:RE = 1.2-2.8%	5 h/30 h
Cerebral blood flow estimation (Galazis et al., 2025)	Least squares fitting	CBF:RE = -0.3 ± 71.7, AT:RE = 30.5 ± 257.8, T_{1b} :RE = -4.4 ± 28.9 nCBF: r = 0.84 ± 0.03, nCBV: r = 0.92 ± 0.03	73.3 min/5.5 s
Contrast perfusion MRI (Rotkopf et al., 2024)	In vivo dataset	ω :RE = 15.0 ± 0.1%, Q : RE = 6.6 ± 4.7%	161 ± 15 s
Cerebrovascular quantification (Ferdian et al., 2023)	Synthetic data	C :RE = 7.98 ± 1.08-74.64 ± 11.07	N/A
Three-element Windkessel parameters (Garay et al., 2024)	FEM		10 min-27 h 54 min
murine perivascular flows quantification (Boster et al., 2023)	PTV	ω :RE = 16.33 ± 11.09, p :RE = -2.75 ± 2.01, WSS: RE = 3.00 ± 1.45 × 10 ⁻³	N/A
Cuffless blood pressure estimation (Sel et al., 2023)	Monitoring device	systolic: RE = 1.3 ± 7.6, diastolic: RE = 0.6 ± 6.4	N/A
4D flow MRI resolution (Fathi et al., 2020)	PIV	ASI: Q_1 = 0.97, MSI: Q_1 = 0.89, SI: Q_1 = 0.86	N/A

Abbreviations: RE, relative error; L_2 , L_2 error norm; N/A, not applicable; RMSE, root mean square error; RAE, relative absolute error; R^2 , correlation coefficient; r, Pearson's correlation coefficient; FFR, fractional flow reserve; CBF, cerebral blood flow; AT, bolus arrival time; T_{1b} , blood longitudinal relaxation time; nCBF, normalized cerebral blood flow; nCBV, normalized cerebral blood volume; C, vessel compliance; PTV, particle tracking velocimetry; PIV, particle image velocimetry; ASI, angular similarity index; MSI, magnitude similarity index; SI, similarity index; Q_1 , First quartile.

Furthermore, Table 2 summarizes the performance of PINNs applied to a wide range of blood flow simulation problems across different vascular regions and modalities. Accuracy was generally assessed relative to conventional reference methods including CFD, FEM, in vivo data, and medical imaging, with most studies reporting low relative errors (typically < 10%) or strong correlation coefficients ($R^2 > 0.8$). Computational efficiency varied substantially, ranging from seconds to several days depending on problem scale and complexity, highlighting both the potential and current challenges of PINNs in balancing accuracy with computational cost. Overall, these results demonstrate the versatility of PINNs in simulating and inferring hemodynamic parameters, while underscoring the need for further optimization in large-scale or patient-specific applications.

To support further development and implementation, Table 3 lists a selection of publicly available code repositories specifically related to PINNs-based hemodynamic analysis. These resources provide baseline implementations, reproducible workflows, and customizable architectures for various cardiovascular applications. Besides, Table 4 summarizes a set of open-source platforms and toolkits dedicated to hemodynamic modeling and simulation, including software for image-based modeling, CFD solvers, and numerical PDE frameworks that can be seamlessly integrated with PINNs. Collectively, these tools provide a foundation for accelerated research and innovation, enabling the practical application of PINNs in real-world clinical and research settings.

3.1. General blood flow simulation

In recent times, PINNs have emerged as a promising alternative to traditional numerical methods in hemodynamics, owing to mesh-free nature and inherent enforcement of physical laws. These characteristics make PINNs particularly well-suited for simulating blood flow variables and dynamics in both arterial and venous systems. In contrast to conventional numerical methods, PINNs facilitate efficient and adaptable modeling, particularly under conditions of limited or noisy data.

As shown in Fig. 4(a) and (c), Liu et al. (2024) use variable separated PINNs to predict 3D scalar blood flow variables, demonstrating improved prediction accuracy and generalization potential for cardiovascular disease applications. Similarly, Zhang and Tai (2024) employed PINNs to simulate 3D blood flow in elastic vessels with varying degrees of curvature, revealing that highly curved vessels lead to a substantial reduction in fluid velocity and display non-linear diminished activity during the diastolic phase.

Despite these promising results, 3D PINNs-based simulations are computationally intensive due to the high dimensionality and complex geometries involved. To mitigate this, simplified 1D model depicted in Fig. 4(b) can be employed. Assuming the vessel is a straight cylinder along the x-direction and the blood pressure and flow rate are constant within the cross section, the blood flow in the arteries can be reduced

Table 3
Publicly available PINNs code repositories for hemodynamic modeling.

Index	Repository URL	Reference
1	https://github.com/satyasaran/BurgerEvoPINN.git	Bhaumik et al. (2024)
2	https://github.com/Zzzz-Jonathan/FPDE	Zhang et al. (2024b)
3	https://github.com/amir-cardiolab/PINN-wss	Arzani et al. (2021)
4	https://github.com/shengzesnail/AIV_MAOC	Cai et al. (2021a)
5	https://github.com/risc-mi/pinn-blood-flow	Moser et al. (2023)
6	https://github.com/liangbright/DNN_FEM_Integration	Liang et al. (2023)
7	https://github.com/Owais-Khan/CardiovascularPINNs	Aghaei and Khan (2025)
8	https://github.com/ahmetsenemse/PIGNN-1D-Blood-Flow-Simulation	Sen et al. (2024)
9	https://doi.org/10.5281/zenodo.8121537	Zhang et al. (2023)
10	https://github.com/PredictiveIntelligenceLab/1DBloodFlowPINNs	Kissas et al. (2020)
11	https://github.com/sbuoso/Cardio-PINN/	Buoso et al. (2021)
12	https://github.com/HSW15/CSF-PINN	Wong et al. (2025)
13	https://github.com/bmaidu/AIVFM	Maidu et al. (2025)
14	https://github.com/ehsanagh/lpm_pinn	Naghavi et al. (2024)
15	https://github.com/cgalaz01/supinn	Galazis et al. (2025)
16	https://github.com/paulienvoorter/IVIM3brain-NET	Voorster et al. (2023)
17	https://github.com/EdwardFerdian/4DFlowNet	Ferdian et al. (2023)
18	https://github.com/eyemedicen/PINNs-WK-MRI	Garay et al. (2024)
19	https://github.com/dpdclub/Coagulo-net.git	Qian et al. (2024)
20	https://github.com/TAMU-ESP/pinn-for-physiological-timeseries	Sel et al. (2023)
21	https://github.com/paulienvoorter/IVIM-DTI-NET	Voorster et al. (2025)

Table 4
Representative open-source resources for hemodynamic modeling and simulation.

Resource name	Features	Website
SimVascular	Complete pipeline for image-based modeling and simulation	https://simvascular.github.io
OpenFOAM	Versatile CFD platform with customizable solvers	https://www.openfoam.com
FEniCS	High-level Python interface for solving PDEs via FEM	https://fenicsproject.org
CRIMSON	Integrated environment for cardiovascular flow simulation	https://www.crimson.software

to 1D Navier–Stokes equations (Li et al., 2024)

$$\frac{\partial A}{\partial t} + \frac{\partial Q}{\partial x} = 0 \quad (14)$$

$$\frac{\partial Q}{\partial t} + \frac{\partial}{\partial x} \left(\frac{Q^2}{A} \right) + \frac{A}{\rho} \frac{\partial p}{\partial x} + \frac{K_r Q}{A} = 0 \quad (15)$$

where K_r is a resistance parameter related to blood viscosity, Q is the flow rate, and A is the area of cross section.

For 1D hemodynamic models, approximate analytical solutions can be derived using methods such as the reductive perturbation approach (Bhaumik et al., 2024). In most practical applications, however, 1D models are solved numerically, which offers an effective compromise between computational efficiency and physiological accuracy. The simplified 1D models have been effectively utilized to study various scenarios, such as the periodicity of blood flow (Li et al., 2024) shown in Fig. 4(d), the dynamics of nonlinear pulse propagation through visco-elastic tubes (Bhaumik et al., 2024) and blood flow in bifurcation arteries (Chang et al., 2024). By substantially reducing computational costs while preserving essential flow characteristics, 1D models are particularly suitable for large-scale or time-sensitive simulations. Nevertheless, simplified 1D models remain limited in capturing detailed interactions between blood flow and vascular wall mechanics. Therefore, the choice between 1D and more sophisticated 3D models should be guided by the specific physiological context and the required resolution of the simulation.

3.2. Stenosis and aneurysm

Arterial diseases such as stenosis and aneurysm are closely linked to localized alterations in hemodynamic forces and the formation of complex flow patterns, particularly in regions of geometric irregularity such as vessel curvatures, luminal constrictions, and bulges. PINNs have shown considerable potential for modeling blood flow and wall interactions in these anatomically and clinically significant areas.

A number of studies have demonstrated the application of PINNs in idealized models of stenosis and aneurysm. Arzani et al. (2021) employed PINNs to estimate near-wall flow velocity and WSS using sparse velocity data, without requiring explicit inlet or outlet boundary conditions. Cai et al. (2021a) introduced an artificial intelligence velocimetry (AIV) approach that integrates imaging data with governing equations via PINNs to quantify velocity and stress distributions in microchannels mimicking saccular microaneurysms, as shown in Fig. 5(a). While this represents a successful integration of experimental and computational domains, scaling the method to larger and more anatomically accurate vascular geometries remains an open challenge. Additionally, Shi et al. (2024) developed a robust multiphysics PINNs-based surrogate model for predicting in-stent restenosis, incorporating both biological constraints and drug elution dynamics. Despite its conceptual novelty, the model's validation against *in vivo* data or clinical outcomes has yet to be fully explored.

Recent efforts have moved toward more clinically relevant, patient-specific geometries. For example, Liu et al. (2025) proposed an integral conservation PINNs with adaptive activation functions for estimating velocity, pressure, and WSS in stenotic and aneurysmal vessels, without relying on high-fidelity simulation data. The proposed framework showed strong performance across multiple geometric scenarios, as illustrated in Fig. 5(b) and (c). However, most models rely on assumptions of laminar flow and Newtonian fluid behavior, which may not hold in highly disturbed or pulsatile regimes. Moser et al. (2023) conducted a comparative study of various neural network architectures, assessing their accuracy and computational efficiency. The results indicated that FNN achieved a favorable balance between performance and training time, whereas more sophisticated architectures provided improved accuracy, particularly in simple geometries. However, in more complex aneurysmal geometries, prediction accuracy declined.

3.3. Aortic hemodynamics

As the primary conduit for blood ejected from the heart, the aorta plays a central role in systemic hemodynamics and is a key target

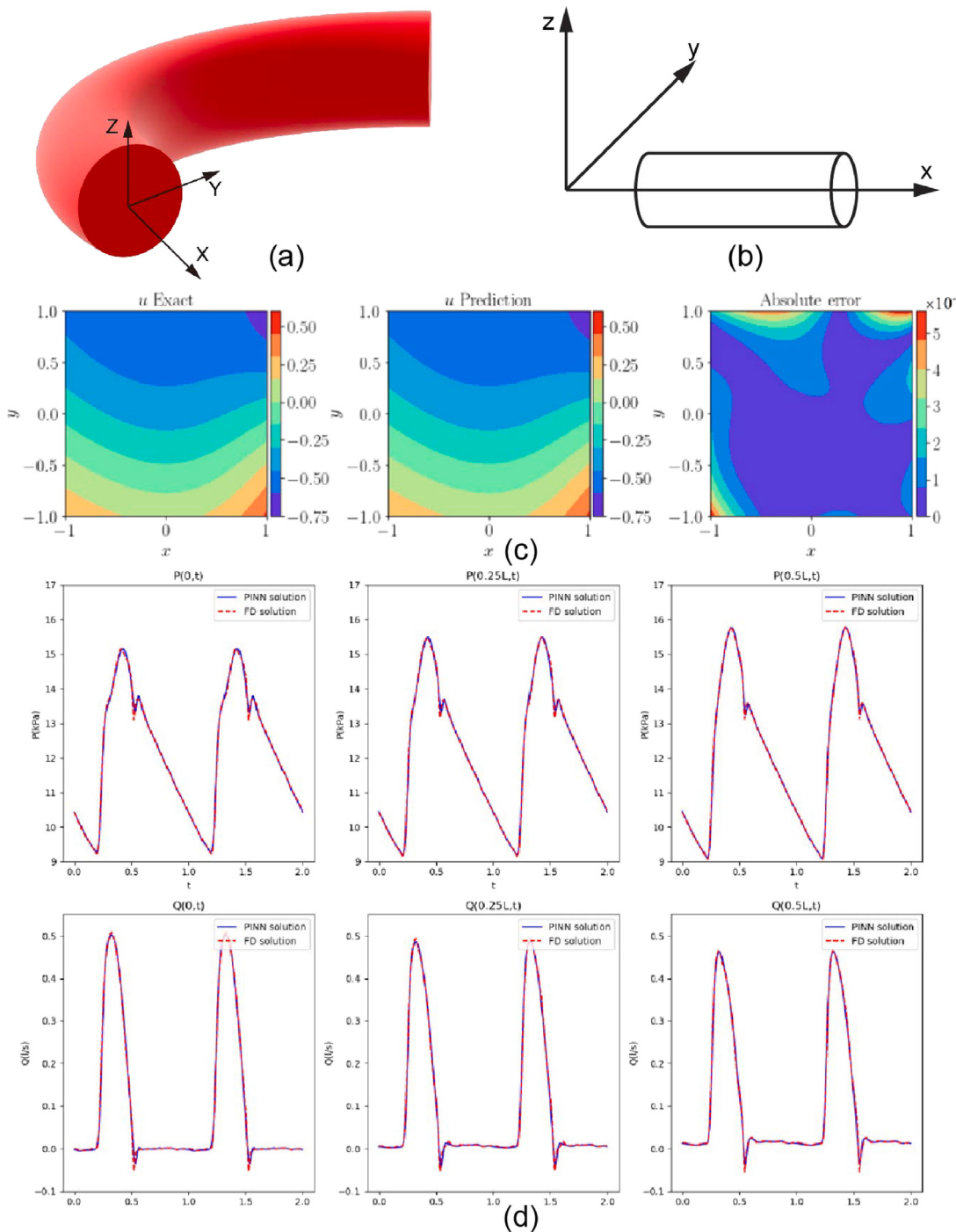


Fig. 4. Applications of PINNs in general blood flow simulation: (a) 3D blood vessel configuration. (b) Reduction of the 3D model to a 1D formulation. (c) Snapshot of the velocity fields obtained from PINNs with analytical solutions at time $t = 1$ on the plane $z = 0$ (Liu et al., 2024). Copyright 2023. Elsevier. (d) Comparison of pressure and flow rate between PINN solution and MacCormack finite difference scheme (Li et al., 2024). Copyright 2024. Elsevier.

for predictive modeling in cardiovascular research. PINNs have been increasingly applied to simulate aortic hemodynamics by combining patient-specific anatomical data with physical constraints derived from governing equations.

Aghaee and Khan (2024, 2025) evaluated Fourier-based activation functions in PINNs and found improved convergence and spectral performance under pulsatile flow, though accuracy diminished in turbulent-like conditions with errors rising beyond 50% for high-severity aortic stenoses. To better represent vascular topology and network-level hemodynamics, Sen et al. (2024) introduced physics-informed graph neural networks to solve 1D blood flow equations

across aorta vascular networks, showing strong agreement with numerical solvers and good generalizability to *in vivo* data.

Moreover, Zhang et al. (2023) explored optimal PINNs architectures for four dimensions (4D) hemodynamic predictions in various aortic geometries using point cloud data, demonstrating high scalability and improved accuracy for morphologically complex aorta vessels in Fig. 6(a). Kang et al. (2024) further combined PINNs with PointNet and quadratic residual networks to predict hemodynamics in abdominal aortic aneurysms following endovascular aneurysm repair, reducing computation time drastically while maintaining clinical-level precision. As shown in Fig. 6(b), Ur Rehman et al. (2025) applied PINNs to four

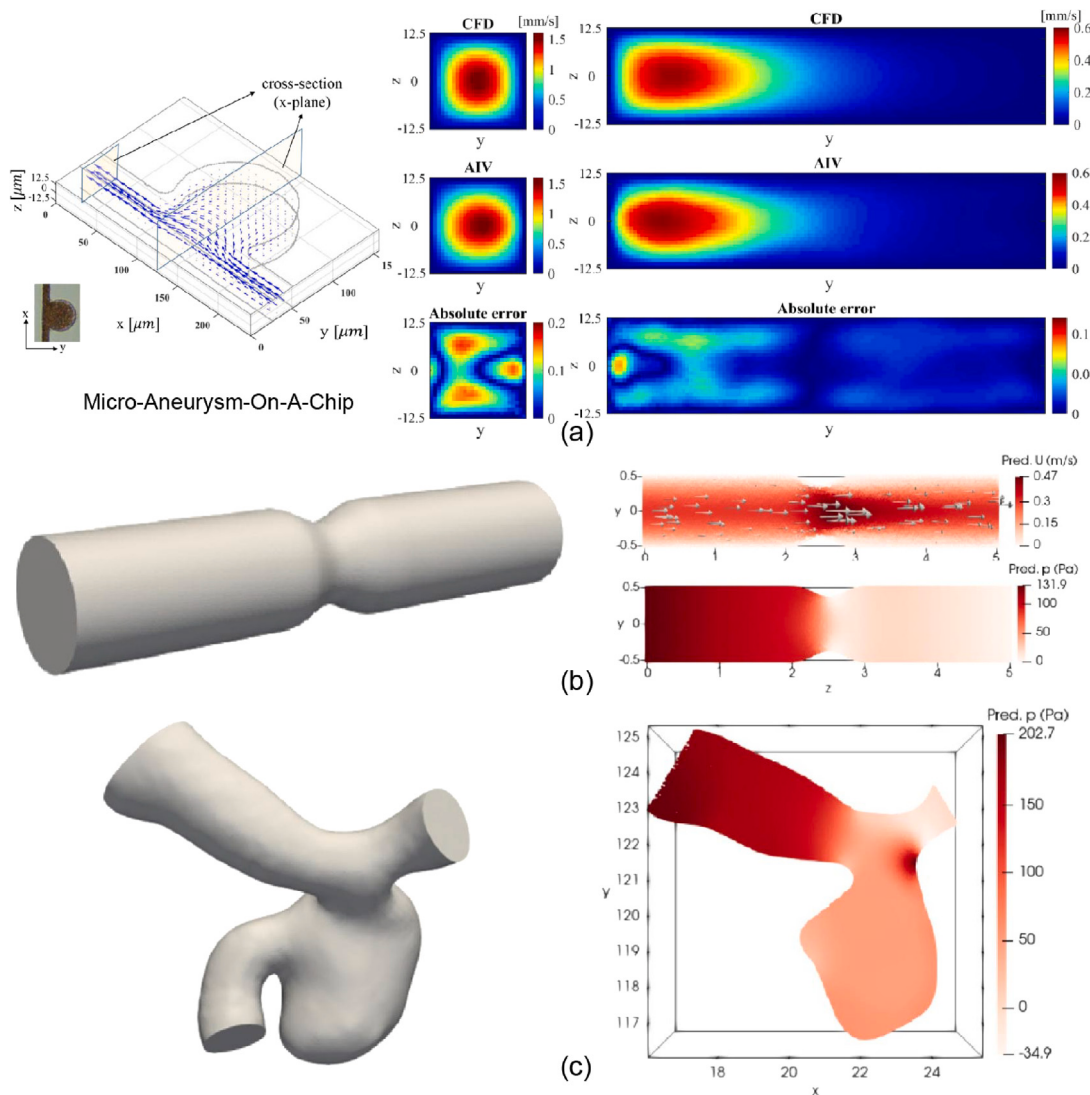


Fig. 5. Applications of PINNs in stenosis and aneurysm modeling: (a) Comparison of 3D AIV predictions with results of CFD simulations for the Micro-Aneurysm-On-A-Chip channel with body-to-neck ratio = 5 (Cai et al., 2021a). Copyright 2021. S. Cai et al. (b) Predicted velocity and pressure distributions from PINNs in a 3D stenosis model (Liu et al., 2025). Copyright 2025. Elsevier. (c) Predicted pressure slice from a 3D aneurysm model using PINNs (Liu et al., 2025). Copyright 2025. Elsevier.

Marfan syndrome-affected and two healthy aortic models, demonstrating strong agreement with conventional CFD results while significantly reducing computational costs. Their findings emphasized the importance of WSS and von Mises stress in assessing aneurysm progression and rupture risk. However, validation was limited to a small cohort and did not include long-term clinical outcome data.

3.4. Cardiac hemodynamics

Cardiac hemodynamics involves the analysis of blood flow and pressure dynamics within the heart chambers and across cardiac valves. Among the most compelling applications of PINNs is the accurate reconstruction of intraventricular flow and myocardial mechanics, which is essential for the diagnosis and monitoring of heart failure, valvular diseases, and congenital anomalies.

One notable application involves the modeling of flow downstream of a transcatheter aortic valve implantation (TAVI) device. As illustrated in Fig. 7(a), Oldenburg et al. (2022) applied PINNs to reconstruct velocity and pressure fields in the post-TAVI region, demonstrating strong agreement with CFD simulations while offering computational advantages. Buoso et al. (2021) proposed a parametric PINNs

framework constrained by hyperelastic energy functionals to simulate patient-specific left ventricular deformation, which achieved over a 30-fold speedup compared to traditional FEM, with only minor compromises in accuracy. Wong et al. (2025) introduced a coupled sequential frame PINNs (CSF-PINNs) that reconstructs intraventricular pressure and velocity fields from Doppler ultrasound, capturing detailed features such as vortical structures and pressure gradients even under noisy input conditions, as illustrated in Fig. 7(c). This demonstrates the robustness of PINNs for clinical echocardiography applications, yet the method still requires careful temporal alignment of imaging frames and may be sensitive to errors in ultrasound-derived boundary conditions.

Additional innovations of PINNs in cardiac modeling include intraventricular vector flow mapping (Maidu et al., 2025), inverse modeling of myocardial contractility (Naghavi et al., 2024), and hybrid frameworks that integrate PINNs with CFD and fluid-structure interactions (FSI) models for coronary FFR estimation. For example, Alzhanov et al. (2024b,a) estimated FFR throughout the cardiac cycle using a rigid-wall interaction model, as shown in Fig. 7(b), providing a noninvasive alternative to catheter-based FFR measurements. However, rigid-wall assumptions can lead to inaccurate pressure estimations in patients with impaired ventricular compliance or vessel wall abnormalities.

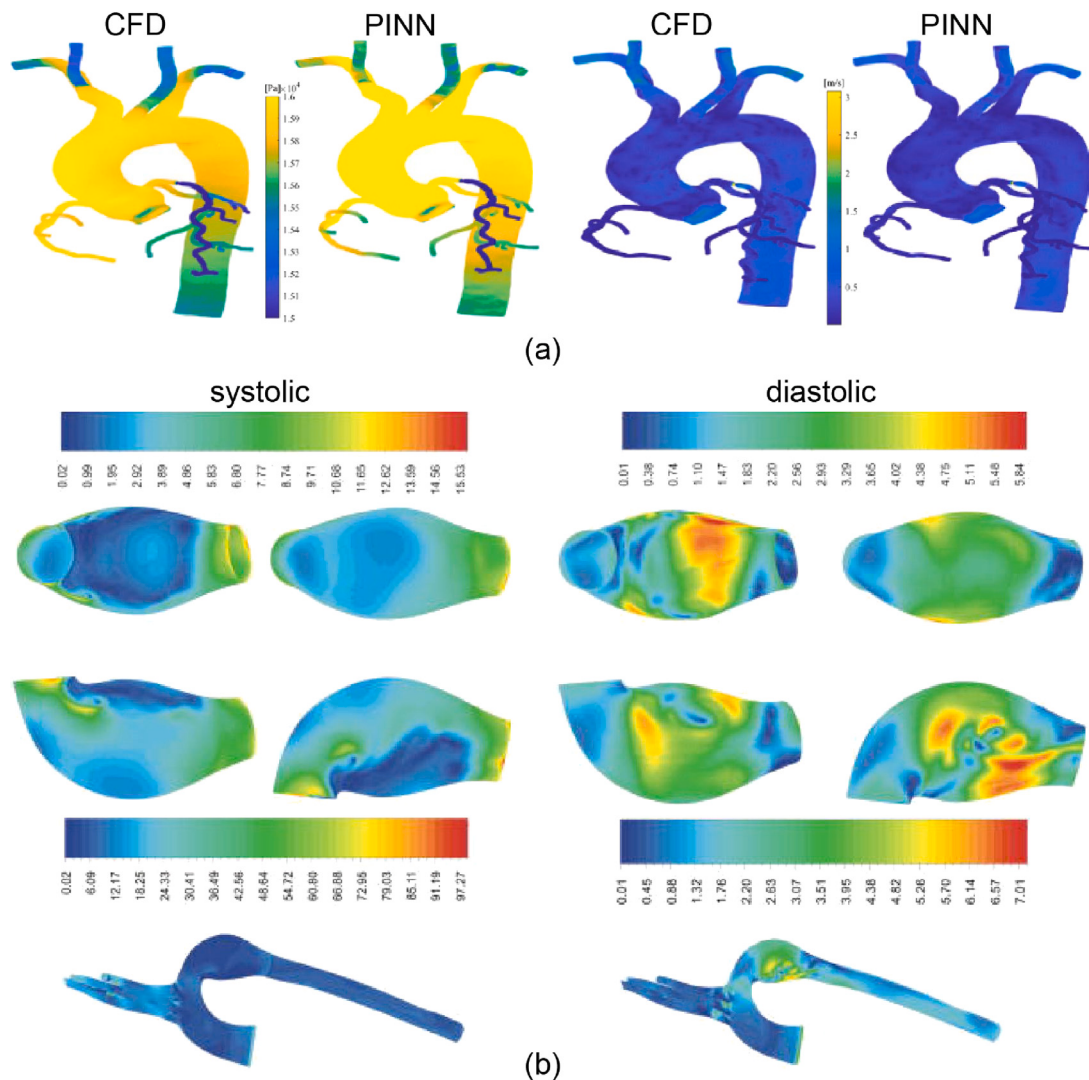


Fig. 6. Applications of PINNs in aortic hemodynamics: (a) Visual comparison of velocity and pressure fields from CFD and PINNs in complex aortic geometry (Zhang et al., 2023). Copyright 2023. Elsevier. (b) PINNs-based WSS and von Mises stress distributions in Marfan syndrome aneurysm models during systolic and diastolic phases (Ur Rehman et al., 2025). Copyright 2025. M. A. Ur Rehman et al..

3.5. Cerebral hemodynamics

Accurate modeling of cerebral blood dynamics is essential for detecting and monitoring pathophysiological changes associated with stroke, small vessel disease, and neurodegenerative conditions. Traditional imaging and modeling approaches often suffer from limited spatial resolution, sensitivity to noise, and lengthy acquisition times, which constrain their clinical applicability.

PINNs have recently gained attraction as a powerful tool for enhancing cerebral hemodynamic modeling, particularly in perfusion and diffusion MRI. As illustrated in Fig. 8(a), Galazis et al. (2025) employed PINNs to estimate cerebral perfusion in neonates, successfully extracting physiological parameters from undersampled MRI data. Similarly, Rotkopf et al. (2024) applied PINNs-based frameworks to dynamic susceptibility contrast (DSC) perfusion MRI and reported improved robustness to noise and more accurate estimation of key hemodynamic parameters, including cerebral blood volume and mean transit time.

In the domain of diffusion MRI, the application of PINNs to multi-b-value and multi-directional data has also shown significant promise. Voorter et al. (2023) and Wang et al. (2024) reported enhanced image quality and more reliable estimation of cerebrovascular parameters

using PINNs-based reconstruction techniques presented in Fig. 8(b). In a subsequent advancement, Voorter et al. (2025) estimated anisotropic pseudo-diffusion (D^*) tensors by leveraging multi-directional, multi-b-value diffusion data. Their approach demonstrated sensitivity to both cerebrospinal fluid and blood flow, enabling the detection of microvascular alterations associated with small vessel disease and aging.

Beyond diffusion and perfusion imaging, PINNs have also been extended to arterial spin labeling (ASL) and 4D-Flow MRI. Ishida et al. (2024a) applied PINNs to enhance parameter estimation in multi-postlabeling delay ASL. As shown in Fig. 8(c), the model improved cerebral blood flow quantification and exhibited robustness to synthetic noise, highlighting its potential for clinical translation. In parallel, Fathi et al. (2020) introduced a PINNs-based approach for super-resolution and denoising of 4D-Flow MRI, yielding more accurate and higher-resolution reconstructions of cerebral velocity fields. However, the performance of the PINNs-based model may degrade in the presence of motion artifacts or low signal-to-noise ratios, which are common in long-duration neurovascular MRI scans.

3.6. Parameter estimation

Accurate parameter estimation is a fundamental challenge in hemodynamics, primarily due to the ill-posed nature of inverse problems

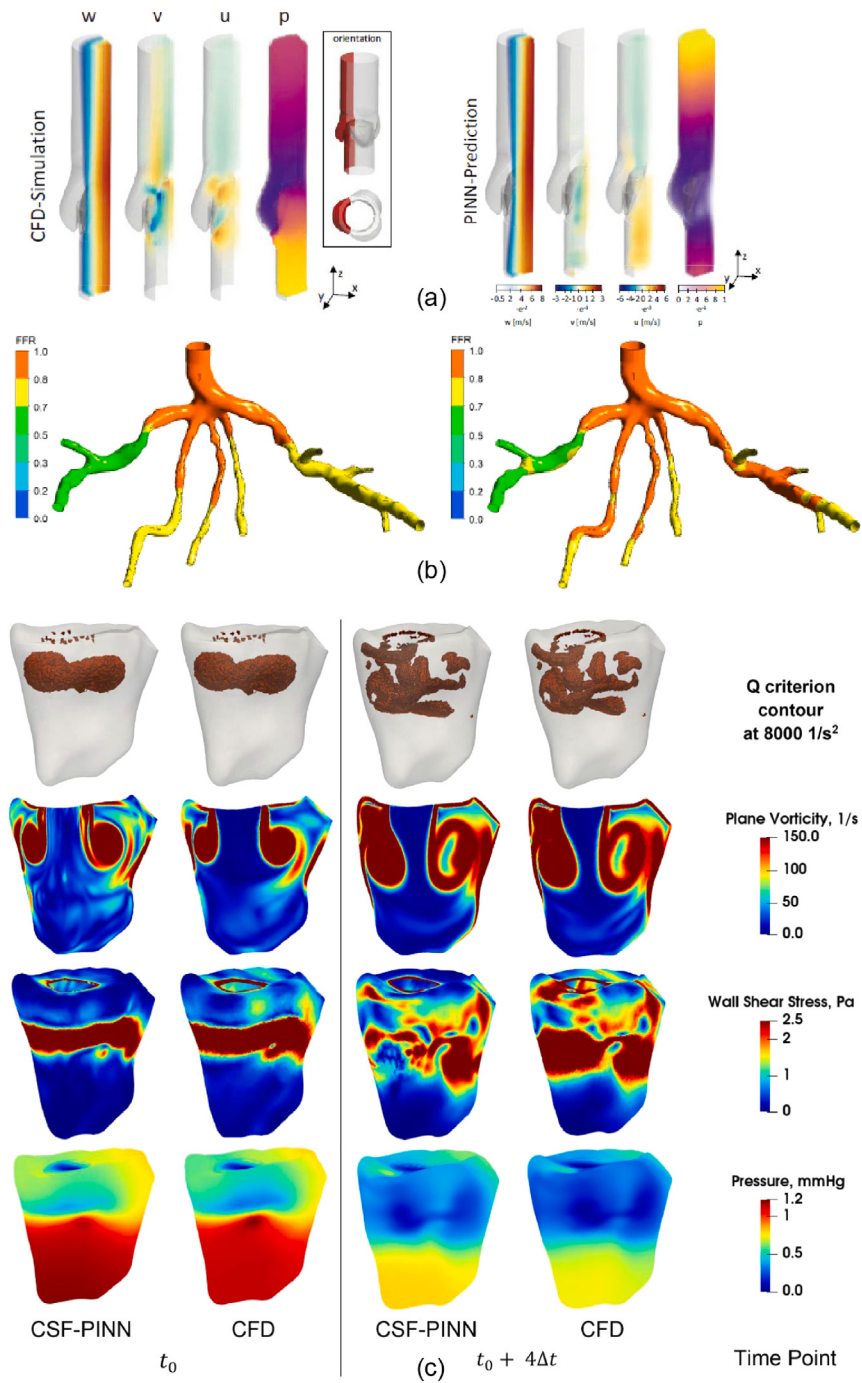


Fig. 7. Applications of PINNs in aortic hemodynamics: (a) Comparison of CFD and PINNs predictions of velocity and pressure downstream of a TAVI device (Oldenburg et al., 2022). Copyright 2022 J. Oldenburg et al. (b) FFR distribution in CT209 coronary artery throughout systolic and diastolic phases of the cardiac cycle with rigid FSI interaction (Alzhanov et al., 2024a). Copyright 2024 N. Alzhanov et al. (c) Hemodynamic metrics (velocity, pressure) reconstructed by CSF-PINN compared to CFD benchmarks (Wong et al., 2025). Copyright 2025 H. S. Wong et al..

and the sparse, noisy nature of clinical measurement data. To address these issues, PINNs have emerged as a powerful framework that integrates governing physical laws, such as the Navier-Stokes equations and mass conservation into the neural network training process. This integration improves robustness, reduces overfitting, and enables reliable estimation of physiological parameters even under data-constrained conditions. Recent studies have demonstrated the versatility and accuracy of PINNs in a variety of parameter estimation tasks, spanning cardiovascular flows, medical imaging, and broader physiological systems.

In cardiovascular modeling, PINNs have shown particular strength in estimating key flow parameters. Garay et al. (2024) estimated reduced-order model parameters and reconstructed velocity fields in the aorta from noisy 2D data illustrated in Fig. 9(a), showing PINNs outperform Kalman filters, particularly as parameter dimensionality increases. Isaev et al. (2024) estimated inlet/outlet boundary conditions in a Fontan geometry using synthetic data and Latin hypercube sampling, highlighting the impact of physical regularization on estimation accuracy. Du et al. (2023) inferred intra-aortic pressure fields by combining PINNs with simulated FSI data, emphasizing sensitivity to input

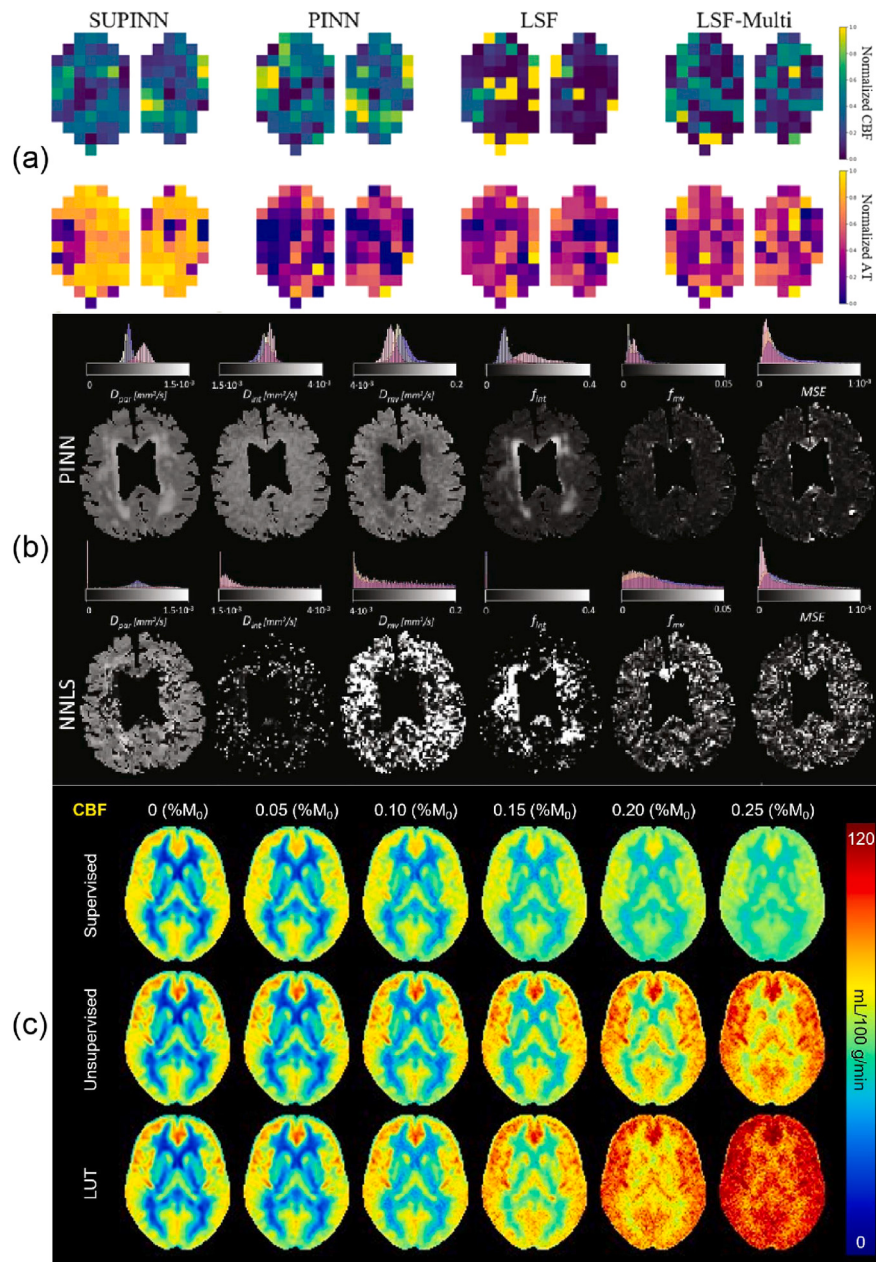


Fig. 8. Applications of PINNs in cerebral hemodynamics: (a) Spatial maps of parameter estimation in deep grey matter for a subject aged 32 weeks (Galazis et al., 2025). Copyright 2025. C. Galazis et al. (b) The corresponding parameter maps and the mean squared error (MSE) of the model fit obtained with PINNs and the non-negative least squares (NNLS) (Voorter et al., 2023). Copyright 2023. P. H. M. Voorter, et al. (c) Averaged parametric maps across subjects predicted from the original and synthesized noisy images (Ishida et al., 2024a). Copyright 2024. S. Ishida et al.

velocity and introducing a novel method for estimating absolute pressure. Boster et al. (2023) integrated sparse velocity measurements with PINNs to quantify the flow of cerebrospinal fluid in pial perivascular spaces.

In medical imaging, PINNs have been applied to estimate physiologically meaningful parameters from non-invasive scans. Ishida et al. (2024b) implemented a physics-informed unsupervised network for multi-delay ASL MRI, yielding noise-robust estimation of cerebral blood flow and arterial transit time. van Herten et al. (2022) used PINNs integrated with a multi-compartment exchange model to estimate myocardial perfusion parameters from cardiac imaging data, achieving lower estimation error compared to traditional kinetic fitting approaches in Fig. 9(b). In positron emission tomography (PET) imaging, Ferrante et al. (2024) introduced a hybrid 3D CNN–PINNs model to estimate

the arterial input function, attaining high correlation with reference values and improving quantification of tracer uptake. Liang et al. (2025) applied PINNs to ultrafast ultrasound velocimetry, achieving high-resolution velocity and pressure field estimates in close agreement with ground truth.

Additionally, PINNs have been successfully extended to multiscale physiological systems. Qian et al. (2024) introduced Coagulo-Net, a PINNs-based model that inferred kinetic parameters of the coagulation cascade from sparse and noisy measurements, enhancing model interpretability and reliability. Sel et al. (2023) developed a PINN model for cuffless blood pressure estimation using wearable bioimpedance signals and physiological constraints, significantly reducing the reliance on labeled data shown in Fig. 9(c). Oszkinat et al. (2023) employed a generative adversarial network augmented PINN framework to estimate

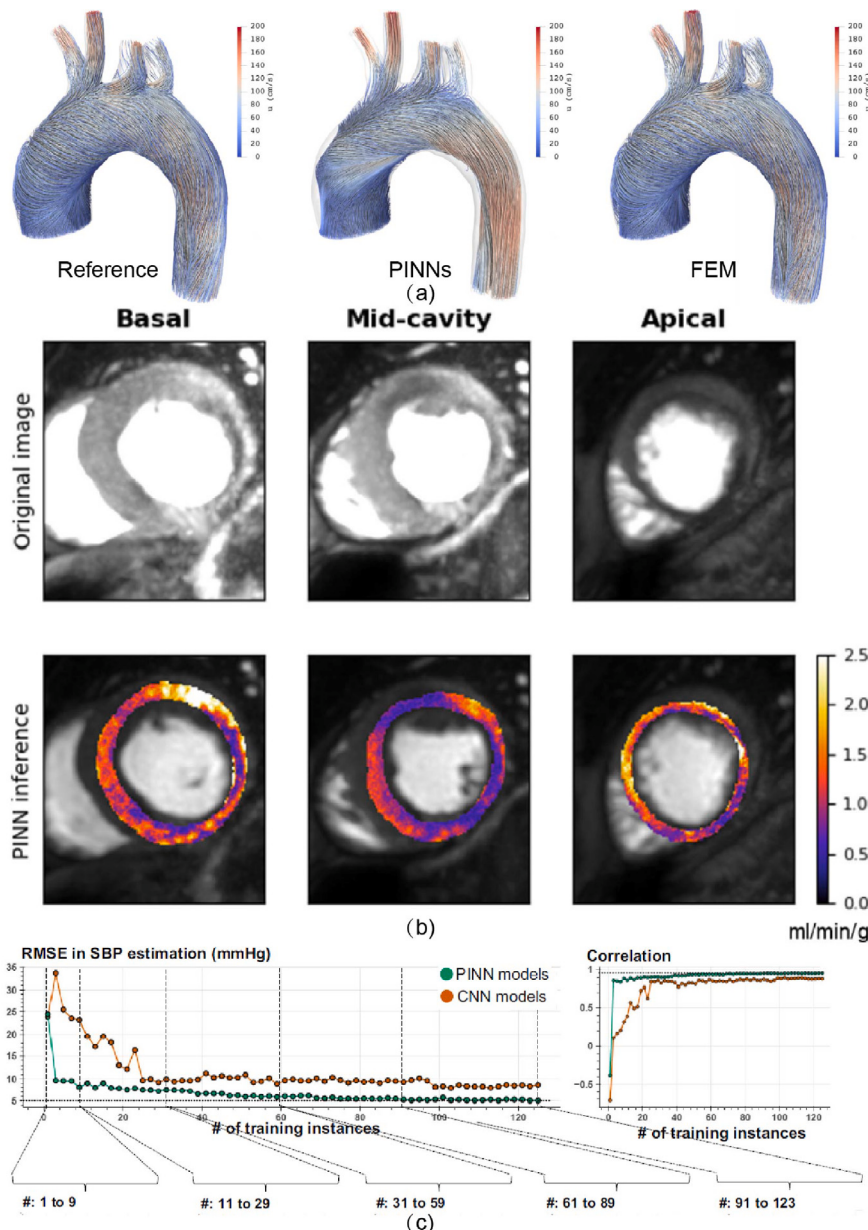


Fig. 9. Applications of PINNs in parameter estimation: (a) Velocity streamlines of the transient aortic flow problem using PINNs-estimated parameters, compared with FEM and reference data (Garay et al., 2024). Copyright 2024. Elsevier. (b) Myocardial blood flow maps estimated via PINNs for a patient with coronary artery disease (van Herten et al., 2022). Copyright 2022. R. L.M. van Herten, et al. (c) RMSE and Pearson correlation for systolic blood pressure estimation by PINN (green) and CNN (orange) under varying labeled data amounts (Sel et al., 2023). Copyright 2023. K. Sel, et al..

blood alcohol concentration from transdermal signals, incorporating diffusion modeling and posterior inference for uncertainty quantification. In neurophysiology, Sotero et al. (2024) applied PINNs to model resting-state functional MRI dynamics, estimating neural model parameters that revealed significant group differences in brain network activity among individuals with autism spectrum disorder. However, the physiological interpretations of these estimated parameters remain speculative without supporting electrophysiological data.

4. Discussion

4.1. Technical limitations

Despite the promise of unifying physics-based modeling with data-driven learning, the application of PINNs in hemodynamic research remains hindered by multiple technical challenges. These limitations

are not confined to numerical efficiency, but extend to issues of validation, robustness, anatomical realism, and scalability, all of which constrain their clinical translation.

The first obstacle lies in validation and benchmarking. Although PINNs are mesh-free and data-efficient, most reported studies still rely heavily on synthetic or simulated datasets. This dependency is not driven by a need for large training sets, as in conventional machine learning, but by the scarcity of high-fidelity physiological measurements such as patient-specific velocity fields or pressure maps. The absence of standardized benchmarks makes it difficult to assess reproducibility and clinical reliability. Addressing this gap will require community-wide efforts to develop standardized validation protocols, including reference geometries, common boundary conditions, and unified error metrics, together with tiered validation strategies encompassing synthetic data, flow phantoms, and advanced imaging modalities such as 4D Flow MRI. Multi-center studies and semi-supervised learning

with partial clinical observations could further enhance robustness and translational relevance.

Equally critical is the sensitivity of PINNs to noise and incomplete data, especially when applied to sparse or imperfect clinical datasets. Unlike conventional CFD, which typically operates with well-defined boundary conditions, PINNs often need to infer these quantities from sparse or incomplete observations, rendering them vulnerable to modality-specific biases and experimental uncertainties. Moreover, the widespread use of MSE loss functions introduces additional fragility, as such losses are poorly suited to handling non-Gaussian noise patterns commonly encountered in clinical data. To enhance robustness and build trust for clinical adoption, future developments should prioritize advanced uncertainty quantification strategies, such as Bayesian PINNs (Yang et al., 2021), ensemble-based methods, and physics-aware noise modeling, that can explicitly account for measurement variability and provide calibrated confidence estimates alongside predictions. Demonstrating these approaches on noisy patient datasets and comparing their performance with deterministic PINNs will be a critical step toward clinical acceptability.

Another major limitation is the difficulty of applying PINNs to anatomically complex, patient-specific vascular models. Current implementations often rely on simplifying assumptions about vascular wall mechanics, constitutive laws, and flow regimes, most commonly treating blood as a Newtonian fluid under laminar conditions. While these approximations facilitate model training, they limit accuracy and generalizability in pathological scenarios such as stenotic jets, aneurysmal recirculation zones, or microvascular networks where turbulence, shear-thinning, and viscoelastic effects play important roles. These oversimplifications reduce the reliability of derived hemodynamic indices, including WSS and pressure gradients, which are critical for clinical decision-making. Future progress will depend on extending PINNs to handle full fluid–structure interaction, non-Newtonian rheology, and time-dependent Navier–Stokes formulations, thereby improving their fidelity and robustness in realistic vascular environments.

Finally, scalability and model reusability remain unresolved. Hyperparameter tuning in PINNs is still largely empirical, with network architecture, loss weighting, and optimization strategy often chosen by trial and error. This is problematic because the balance between data-driven and physics-based loss terms is highly problem-dependent, and poor choices can yield unstable or biased solutions. While adaptive loss balancing (McCleny and Braga-Neto, 2023; Li et al., 2022) and automated architecture search have shown promise, broader frameworks for transfer learning and reusability across patients and imaging settings are still lacking. Such methods are vital if PINNs are to evolve from bespoke research tools into scalable platforms for clinical workflows.

Taken together, these limitations highlight that the current successes of PINNs in hemodynamics are largely confined to controlled, small-scale studies. Overcoming barriers in validation, robustness, realism, and scalability will be decisive for clinical translation. Standardized evaluation pipelines, integration of uncertainty quantification, physiologically accurate modeling, and transferable architectures should therefore be prioritized in the next phase of development.

4.2. Regulatory and translational considerations

Beyond technical challenges, regulatory and translational barriers also shape the clinical trajectory of PINNs. Computational efficiency remains a major concern, as current models often require long training times and specialized hardware, incompatible with the rapid turnaround expected in clinical practice. Real-world deployment will depend on algorithmic innovations that reduce computational burden and deliver predictions in real- or near-real time.

Seamless integration into hospital infrastructure is another critical requirement. PINNs-based tools must operate within existing ecosystems, including picture archiving and communication systems (PACS), imaging modalities (e.g., OCT, MRI), and electronic health records,

without adding complexity for clinicians. Ensuring interoperability will be key to adoption in routine workflows.

Regulatory approval pathways for artificial intelligence systems that embed physical constraints remain underdeveloped. Unlike conventional machine learning models, PINNs combine data-driven learning with physical equations solvers, raising questions about how to certify safety, robustness, and reproducibility under evolving regulatory frameworks. Establishing clear standards for validation, interpretability, and reproducibility will be critical for clinical translation.

Finally, broader considerations such as ethical, legal, and social challenges must also be addressed to foster clinical adoption of PINNs. As discussed by Perc et al. (2019), responsible integration of artificial intelligence into healthcare requires frameworks for transparency and accountability. Complementary studies (İlirkhan et al., 2025) emphasize the need for synergistic use of artificial intelligence with existing clinical workflows to maximize benefit and minimize risks. Addressing these regulatory and translational considerations in parallel with methodological development is essential to ensure that PINNs progress from research prototypes to trustworthy, clinically deployable tools.

5. Conclusion

This study presents a comprehensive review of recent advancements in the application of PINNs to hemodynamic problems. Through the integration of physical laws into the training process, PINNs establish a robust framework for addressing cardiovascular flow problems with improved efficiency and interpretability. The strengths of PINNs are particularly evident in areas including mesh-free simulation, parameter estimation, inverse problem solving, and integration with multi-modal medical imaging data. Therefore, PINNs have been successfully applied across a wide spectrum of hemodynamic scenarios, from large-vessel aortic and cardiac flows to microvascular cerebral perfusion. Comparative studies have demonstrated the capability of PINNs to infer physiologically meaningful parameters under sparse data conditions and to enable patient-specific modeling with promising diagnostic value.

However, several limitations continue to constrain PINNs clinical translation and large-scale deployment. These include the scarcity of high-quality *in vivo* validation data, the lack of robust uncertainty quantification methods, limited generalizability across diverse anatomical geometries and flow regimes, and the absence of standardized strategies for model architecture design and hyperparameter tuning.

Bridging the gap between current studies and real-world clinical application will require multidisciplinary efforts. Future research should prioritize: (1) the development of large-scale, publicly accessible clinical datasets with labeled hemodynamic parameters; (2) rigorous experimental validation using patient-specific imaging and measurements; (3) algorithmic innovations to improve training efficiency, numerical stability, and generalizability; and (4) integration of PINNs into user-friendly pipelines compatible with clinical workflows.

CRediT authorship contribution statement

Xianglong Yu: Writing – original draft, Visualization, Data curation, Conceptualization. **Yu Hu:** Writing – review & editing. **Rui Guo:** Writing – review & editing, Conceptualization. **Lei Fan:** Writing – review & editing, Conceptualization. **Haiyan Ding:** Writing – review & editing, Conceptualization. **Jingjing Xiao:** Writing – review & editing, Supervision, Conceptualization.

Declaration of competing interest

The authors declare that they have no known competing financial interests or personal relationships that could have appeared to influence the work reported in this paper.

Acknowledgments

The authors would like to thank for the support of the Natural Science Foundation of Chongqing, China (CSTB2025NSCQ-GPX0607) and the Young PhD Talents cultivation Project (2024YQB022) of the Second Affiliated Hospital of Army Medical University.

Data availability

No data was used for the research described in the article.

References

- Aghaee, A., Khan, M.O., 2024. Performance of Fourier-based activation function in physics-informed neural networks for patient-specific cardiovascular flows. *Comput. Methods Programs Biomed.* 247, 108081. <http://dx.doi.org/10.1016/j.cmpb.2024.108081>.
- Aghaee, A., Khan, M.O., 2025. Pinning down the accuracy of physics-informed neural networks under laminar and turbulent-like aortic blood flow conditions. *Comput. Biol. Med.* 185, 109528. <http://dx.doi.org/10.1016/j.combiomed.2024.109528>.
- Alzhanov, N., Ng, E.Y.K., Zhao, Y., 2024a. Hybrid CFD PINN FSI simulation in coronary artery trees. *Fluids* 9 (12), 280. <http://dx.doi.org/10.3390/fluids9120280>.
- Alzhanov, N., Ng, E.Y.K., Zhao, Y., 2024b. Three-dimensional physics-informed neural network simulation in coronary artery trees. *Fluids* 9 (7), 153. <http://dx.doi.org/10.3390/fluids9070153>.
- Arzani, A., Wang, J.-X., D'Souza, R.M., 2021. Uncovering near-wall blood flow from sparse data with physics-informed neural networks. *Phys. Fluids* 33 (7), 071905. <http://dx.doi.org/10.1063/5.0055600>.
- Berhane, H., Scott, M., Elbaz, M., Jarvis, K., McCarthy, P., Carr, J., Malaisrie, C., Avery, R., Barker, A.J., Robinson, J.D., Rigsby, C.K., Markl, M., 2020. Fully automated 3D aortic segmentation of 4D flow MRI for hemodynamic analysis using deep learning. *Magn. Reson. Med.* 84 (4), 2204–2218. <http://dx.doi.org/10.1002/mrm.28257>.
- Bhaumik, B., De, S., Changdar, S., 2024. Deep learning based solution of nonlinear partial differential equations arising in the process of arterial blood flow. *Math. Comput. Simulation* 217, 21–36. <http://dx.doi.org/10.1016/j.matcom.2023.10.011>.
- Boster, K.A., Cai, S., Ladrón-De-Guevara, A., Sun, J., Zheng, X., Du, T., Thomas, J.H., Nedergaard, M., Karniadakis, G.E., Kelley, D.H., 2023. Artificial intelligence velocimetry reveals *in vivo* flow rates, pressure gradients, and shear stresses in murine perivascular flows. *Proc. Natl. Acad. Sci. USA* 120 (14), e2217744120. <http://dx.doi.org/10.1073/pnas.2217744120>.
- Buoso, S., Joyce, T., Kozerke, S., 2021. Personalising left-ventricular biophysical models of the heart using parametric physics-informed neural networks. *Med. Image Anal.* 71, 102066. <http://dx.doi.org/10.1016/j.media.2021.102066>.
- Cai, S., Li, H., Zheng, F., Kong, F., Dao, M., Karniadakis, G.E., Suresh, S., 2021a. Artificial intelligence velocimetry and microaneurysm-on-a-chip for three-dimensional analysis of blood flow in physiology and disease. *Proc. Natl. Acad. Sci. USA* 118 (13), e2100697118. <http://dx.doi.org/10.1073/PNAS.2100697118>.
- Cai, S., Mao, Z., Wang, Z., Yin, M., Karniadakis, G.E., 2021b. Physics-informed neural networks (PINNs) for fluid mechanics: a review. *Acta Mech. Sinica/Lixue Xuebao* 37 (12), 1727–1738. <http://dx.doi.org/10.1007/s10409-021-01148-1>.
- Chang, Y.-C., Lin, Y.-S., Hu, J.-J., 2024. Physics-informed neural networks for solving blood flows. In: 2024 26th International Conference on Advanced Communications Technologies. ICACT, pp. 1–4. <http://dx.doi.org/10.23919/ICACT60172.2024.10471938>.
- Changdar, S., Bhaumik, B., Sadhukhan, N., Pandey, S., Mukhopadhyay, S., De, S., Bakalis, S., 2024. Integrating symbolic regression with physics-informed neural networks for simulating nonlinear wave dynamics in arterial blood flow. *Phys. Fluids* 36 (12), 121924. <http://dx.doi.org/10.1063/5.0247888>.
- Chen, Z., Liu, J., Wang, A., Wu, B., Cheng, Z., Jiang, Y., Gu, H., Ding, L., Mo, J., Jiang, Y., Liu, L., Jing, L., Jing, J., Wang, Y., Zhao, X., Wang, Y., Qin, H., Li, Z., 2024. Hemodynamic impairment of blood pressure and stroke mechanisms in symptomatic intracranial atherosclerotic stenosis. *Stroke* 55 (7), 1798–1807. <http://dx.doi.org/10.1161/STROKEAHA.123.046051>.
- Chiu, P.-H., Wong, J.C., Ooi, C., Dao, M.H., Ong, Y.-S., 2022. CAN-PINN: A fast physics-informed neural network based on coupled-automatic-numerical differentiation method. *Comput. Methods Appl. Mech. Engrg.* 395, 114909. <http://dx.doi.org/10.1016/j.cma.2022.114909>.
- Dobroserdova, T.K., Isaev, A.A., Danilov, A.A., Simakov, S.S., 2024. Junction conditions for one-dimensional network hemodynamic model for total cavopulmonary connection using physically informed deep learning technique. *Russian J. Numer. Anal. Math. Modelling* 39 (5), 259–271. <http://dx.doi.org/10.1515/rnam-2024-0023>.
- Du, M., Zhang, C., Xie, S., Pu, F., Zhang, D., Li, D., 2023. Investigation on aortic hemodynamics based on physics-informed neural network. *Math. Biosci. Eng.* 20 (7), 11545–11567. <http://dx.doi.org/10.3934/mbe.2023512>.
- Farrag, A., Yang, Y., Cao, N., Won, D., Jin, Y., 2025. Physics-informed machine learning for metal additive manufacturing. *Prog. Addit. Manuf.* 10 (1), 171–185. <http://dx.doi.org/10.1007/s40964-024-00612-1>.
- Fathi, M.F., Perez-Raya, I., Baghaie, A., Berg, P., Janiga, G., Arzani, A., D'Souza, R.M., 2020. Super-resolution and denoising of 4D-flow MRI using physics-informed deep neural nets. *Comput. Methods Programs Biomed.* 197, 105729. <http://dx.doi.org/10.1016/j.cmpb.2020.105729>.
- Ferdian, E., Marlevi, D., Schollenberger, J., Aristova, M., Edelman, E., Schnell, S., Figueiroa, C., Nordsletten, D., Young, A., 2023. Cerebrovascular super-resolution 4D flow MRI – sequential combination of resolution enhancement by deep learning and physics-informed image processing to non-invasively quantify intracranial velocity, flow, and relative pressure. *Med. Image Anal.* 88, 102831. <http://dx.doi.org/10.1016/j.media.2023.102831>.
- Ferrante, M., Inglese, M., Brusaferri, L., Whitehead, A.C., Macchioni, L., Turkheimer, F.E., Nettis, M.A., Mondelli, V., Howes, O., Loggia, M.L., Veronese, M., Toschi, N., 2024. Physically informed deep neural networks for metabolite-corrected plasma input function estimation in dynamic PET imaging. *Comput. Methods Programs Biomed.* 256, <http://dx.doi.org/10.1016/j.cmpb.2024.108375>.
- Galazis, C., Chiu, C.-E., Arichi, T., Bharath, A.A., Varela, M., 2025. PINNING cerebral blood flow: Analysis of perfusion MRI in infants using physics-informed neural networks. *Front. Netw. Physiol.* 5, <http://dx.doi.org/10.3389/fneph.2025.1488349>.
- Gao, H., Sun, L., Wang, J.-X., 2021. PhyGeoNet: Physics-informed geometry-adaptive convolutional neural networks for solving parameterized steady-state PDEs on irregular domain. *J. Comput. Phys.* 428, 110079. <http://dx.doi.org/10.1016/j.jcp.2020.110079>.
- Garay, J., Dunstan, J., Uribe, S., Sahli Costabal, F., 2024. Physics-informed neural networks for parameter estimation in blood flow models. *Comput. Biol. Med.* 178, 108706. <http://dx.doi.org/10.1016/j.combiomed.2024.108706>.
- Gijssen, F., Katagiri, Y., Barlis, P., Bourantas, C., Collet, C., Coskun, U., Daemen, J., Dijkstra, J., Edelman, E., Evans, P., Van Der Heiden, K., Hose, R., Koo, B.-K., Krams, R., Marsden, A., Migliavacca, F., Onuma, Y., Ooi, A., Poon, E., Samady, H., Stone, P., Takahashi, K., Tang, D., Thondapu, V., Tenekcioglu, E., Timmins, L., Torii, R., Wentzel, J., Serruys, P., 2019. Expert recommendations on the assessment of wall shear stress in human coronary arteries: Existing methodologies, technical considerations, and clinical applications. *Eur. Heart J.* 40 (41), 3421–3433. <http://dx.doi.org/10.1093/eurheartj/ehz551>.
- Gu, L., Qin, S., Xu, L., Chen, R., 2024. Physics-informed neural networks with domain decomposition for the incompressible Navier-Stokes equations. *Phys. Fluids* 36 (2), 021914. <http://dx.doi.org/10.1063/5.0188830>.
- Guo, R., Weingärtner, S., Siurytē, P., Stoeck, C., Füetterer, M., E. Campbell-Washburn, A., Suinesiaputra, A., Jerosch-Herold, M., Nezafat, R., 2022. Emerging techniques in cardiac magnetic resonance imaging. *J. Magn. Reson. Imaging* 55 (4), 1043–1059. <http://dx.doi.org/10.1002/jmri.27848>.
- Heger, P., Hilger, D., Full, M., Hosters, N., 2024. Investigation of physics-informed deep learning for the prediction of parametric, three-dimensional flow based on boundary data. *Comput. Fluids* 278, 106302. <http://dx.doi.org/10.1016/j.compfluid.2024.106302>.
- Hu, H., Qi, L., Chao, X., 2024. Physics-informed neural networks (PINN) for computational solid mechanics: Numerical frameworks and applications. *Thin-Walled Struct.* 205, 112495. <http://dx.doi.org/10.1016/j.tws.2024.112495>.
- İlikhan, S.U., Özer, M., Perc, M., Tanberkan, H., Ayhan, Y., 2025. Complementary use of artificial intelligence in healthcare. *Med. J. West. Black Sea* 9 (1), 7–17.
- Isaev, A., Dobroserdova, T., Danilov, A., Simakov, S., 2024. Physically informed deep learning technique for estimating blood flow parameters in four-vessel junction after the fontan procedure. *Computation* 12 (3), 41. <http://dx.doi.org/10.3390/computation12030041>.
- Ishida, S., Fujiwara, Y., Matta, Y., Takei, N., Kanamoto, M., Kimura, H., Tsujikawa, T., 2024a. Enhanced parameter estimation in multiparametric arterial spin labeling using artificial neural networks. *Magn. Reson. Med.* 92 (5), 2163–2180. <http://dx.doi.org/10.1002/mrm.30184>.
- Ishida, S., Fujiwara, Y., Takei, N., Kimura, H., Tsujikawa, T., 2024b. Comparison between supervised and physics-informed unsupervised deep neural networks for estimating cerebral perfusion using multi-delay arterial spin labeling MRI. *NMR Biomed.* 37 (10), e5177. <http://dx.doi.org/10.1002/nbm.5177>.
- Jagtap, A.D., Kawaguchi, K., Karniadakis, G.E., 2020. Adaptive activation functions accelerate convergence in deep and physics-informed neural networks. *J. Comput. Phys.* 404, 109136. <http://dx.doi.org/10.1016/j.jcp.2019.109136>.
- Kang, J., Li, G., Che, Y., Cao, X., Wan, M., Zhu, J., Luo, M., Zhang, X., 2024. Four-dimensional hemodynamic prediction of abdominal aortic aneurysms following endovascular aneurysm repair combining physics-informed PointNet and quadratic residual networks. *Phys. Fluids* 36 (8), 081904. <http://dx.doi.org/10.1063/5.0220173>.
- Karniadakis, G.E., Kevrekidis, I.G., Lu, L., Perdikaris, P., Wang, S., Yang, L., 2021. Physics-informed machine learning. *Nat. Rev. Phys.* 3 (6), 422–440. <http://dx.doi.org/10.1038/s42254-021-00314-5>.
- Kazi, D.S., Elkind, M.S., Deutsch, A., Dowd, W.N., Heidenreich, P., Khavjou, O., Mark, D., Mussolini, M.E., Ovbiagale, B., Patel, S.S., Poudel, R., Weittenhiller, B., Powell-Wiley, T.M., Joynt Maddox, K.E., Das, S.R., Magnuson, E.A., Pandya, A., Sandhu, A.T., Wasfy, J.H., 2024. Forecasting the economic burden of cardiovascular disease and stroke in the United States through 2050: A presidential advisory from

- the American heart association. *Circulation* 150 (4), e89 – e101. <http://dx.doi.org/10.1161/CIR.0000000000001258>.
- Kharazmi, E., Zhang, Z., Karniadakis, G.E., 2021. Hp-VPINNs: Variational physics-informed neural networks with domain decomposition. *Comput. Methods Appl. Mech. Engrg.* 374, 113547. <http://dx.doi.org/10.1016/j.cma.2020.113547>.
- Kissas, G., Yang, Y., Hwuang, E., Witschey, W.R., Detre, J.A., Perdikaris, P., 2020. Machine learning in cardiovascular flows modeling: Predicting arterial blood pressure from non-invasive 4D flow MRI data using physics-informed neural networks. *Comput. Methods Appl. Mech. Engrg.* 358, 112623. <http://dx.doi.org/10.1016/j.cma.2019.112623>.
- Larson, R.G., Wei, Y., 2019. A review of thixotropy and its rheological modeling. *J. Rheol.* 63 (3), 477–501. <http://dx.doi.org/10.1122/1.5055031>.
- Li, J., Chen, J., Li, B., 2022. Gradient-optimized physics-informed neural networks (GOPINNs): A deep learning method for solving the complex modified KdV equation. *Nonlinear Dynam.* 107 (1), 781–792. <http://dx.doi.org/10.1007/s11071-021-06996-x>.
- Li, L., Tai, X.-C., Chan, R.H.-F., 2024. A new method to compute the blood flow equations using the physics-informed neural operator. *J. Comput. Phys.* 519, 113380. <http://dx.doi.org/10.1016/j.jcp.2024.113380>.
- Li, J.-W., Wang, J., Chen, Y., Yang, H., Wang, Y., Wang, X., Xiao, J., Wang, Y., Qian, D., Yu, S., et al., 2025. Longitudinal blood pressure and cardiovascular outcomes in heart failure: An individual patient data pooling analysis of clinical trials. *Eur. J. Hear. Fail.* <http://dx.doi.org/10.1002/ejhf.3706>.
- Liang, L., Liu, M., Elefteriades, J., Sun, W., 2023. Synergistic integration of deep neural networks and finite element method with applications of nonlinear large deformation biomechanics. *Comput. Methods Appl. Mech. Engrg.* 416, 116347. <http://dx.doi.org/10.1016/j.cma.2023.116347>.
- Liang, M., Liu, J., Wang, H., Chu, H., Zhu, M., Jiang, L., Zong, Y., Wan, M., 2025. High-resolution hemodynamic estimation from ultrafast ultrasound image velocimetry using a physics-informed neural network. *Phys. Med. Biol.* 70 (2), 025001. <http://dx.doi.org/10.1088/1361-6560/ada418>.
- Ling, H.J., Bru, S., Puig, J., Vixegi, F., Mendez, S., Nicoud, F., Courand, P.-Y., Bernard, O., Garcia, D., 2024. Physics-guided neural networks for intraventricular vector flow mapping. *IEEE Trans. Ultrason. Ferroelectr. Freq. Control* 71 (11), 1377–1388. <http://dx.doi.org/10.1109/TUFFC.2024.3411718>.
- Liu, Y., Cai, L., Chen, Y., Chen, Q., 2025. ICPINN: Integral conservation physics-informed neural networks based on adaptive activation functions for 3D blood flow simulations. *Comput. Phys. Comm.* 311, 109569. <http://dx.doi.org/10.1016/j.cpc.2025.109569>.
- Liu, Y., Cai, L., Chen, Y., Ma, P., Zhong, Q., 2024. Variable separated physics-informed neural networks based on adaptive weighted loss functions for blood flow model. *Comput. Math. Appl.* 153, 108–122. <http://dx.doi.org/10.1016/j.camwa.2023.11.018>.
- Liu, X., Mo, X., Zhang, H., Yang, G., Shi, C., Hau, W.K., 2021. A 2-year investigation of the impact of the computed tomography-derived fractional flow reserve calculated using a deep learning algorithm on routine decision-making for coronary artery disease management. *Eur. Radiol.* 31 (9), 7039–7046. <http://dx.doi.org/10.1007/s00330-021-07771-7>.
- Lu, L., Jin, P., Pang, G., Zhang, Z., Karniadakis, G.E., 2021a. Learning nonlinear operators via DeepONet based on the universal approximation theorem of operators. *Nat. Mach. Intell.* 3 (3), 218–229. <http://dx.doi.org/10.1038/s42256-021-00302-5>.
- Lu, L., Pestourie, R., Yao, W., Wang, Z., Verdugo, F., Johnson, S.G., 2021b. Physics-informed neural networks with hard constraints for inverse design. *SIAM J. Sci. Comput.* 43 (6), B1105 – B1132. <http://dx.doi.org/10.1137/21M1397908>.
- Maidu, B., Martinez-Legazpi, P., Guerrero-Hurtado, M., Nguyen, C.M., Gonzalo, A., Kahn, A.M., Bermejo, J., Flores, O., del Alamo, J.C., 2025. Super-resolution left ventricular flow and pressure mapping by Navier-Stokes-informed neural networks. *Comput. Biol. Med.* 185, 109476. <http://dx.doi.org/10.1016/j.combiomed.2024.109476>.
- McClelly, L.D., Braga-Neto, U.M., 2023. Self-adaptive physics-informed neural networks. *J. Comput. Phys.* 474, 111722. <http://dx.doi.org/10.1016/j.jcp.2022.111722>.
- Moser, P., Fenzl, W., Thumfart, S., Ganitzer, I., Giretzlehner, M., 2023. Modeling of 3D blood flows with physics-informed neural networks: Comparison of network architectures. *Fluids* 8 (2), 46. <http://dx.doi.org/10.3390/fluids8020046>.
- Mustafa Turkyilmazoglu, A.A., 2025. Sharp interface establishment through slippery fluid in steady exchange flows under stratification. *Comput. Model. Eng. Sci.* 143 (3), 2847–2865. <http://dx.doi.org/10.32604/cmes.2025.068031>.
- Naghavi, E., Wang, H., Fan, L., Choy, J.S., Kassab, G., Baek, S., Lee, L.-C., 2024. Rapid estimation of left ventricular contractility with a physics-informed neural network inverse modeling approach. *Artif. Intell. Med.* 157, 102995. <http://dx.doi.org/10.1016/j.artmed.2024.102995>.
- Oldenburg, J., Borowski, F., Schmitz, K.-P., Stiehm, M., 2022. Computation of flow through TAVI device by means of physics informed neural networks. *Curr. Dir. Biomed. Eng.* 8 (2), 741–744. <http://dx.doi.org/10.1515/cdbme-2022-1189>.
- Oszkinat, C., Luczak, S.E., Rosen, I., 2023. Uncertainty quantification in estimating blood alcohol concentration from transdermal alcohol level with physics-informed neural networks. *IEEE Trans. Neural Netw. Learn. Syst.* 34 (10), 8094–8101. <http://dx.doi.org/10.1109/TNNLS.2022.3140726>.
- Pashaei Kalajahi, A., Csala, H., Mamun, Z.B., Yadav, S., Amili, O., Arzani, A., D'Souza, R.M., 2025. Input parameterized physics informed neural networks for de noising, super-resolution, and imaging artifact mitigation in time resolved three dimensional phase-contrast magnetic resonance imaging. *Eng. Appl. Artif. Intell.* 150, 110600. <http://dx.doi.org/10.1016/j.engappai.2025.110600>.
- Perc, M., Ozer, M., Hojnik, J., 2019. Social and juristic challenges of artificial intelligence. *Palgrave Commun.* 5 (1), 61. <http://dx.doi.org/10.1057/s41599-019-0278-x>.
- Philip, N.T., Patnaik, B., Sudhir, B., 2022. Hemodynamic simulation of abdominal aortic aneurysm on idealised models: Investigation of stress parameters during disease progression. *Comput. Methods Programs Biomed.* 213, 106508. <http://dx.doi.org/10.1016/j.cmpb.2021.106508>.
- Qian, Y., Zhu, G., Zhang, Z., Modepalli, S., Zheng, Y., Zheng, X., Frydman, G., Li, H., 2024. Coagulo-net: Enhancing the mathematical modeling of blood coagulation using physics-informed neural networks. *Neural Netw.* 180, 106732. <http://dx.doi.org/10.1016/j.neunet.2024.106732>.
- Raissi, M., Perdikaris, P., Karniadakis, G., 2019. Physics-informed neural networks: A deep learning framework for solving forward and inverse problems involving nonlinear partial differential equations. *J. Comput. Phys.* 378, 686–707. <http://dx.doi.org/10.1016/j.jcp.2018.10.045>.
- Raissi, M., Yazdani, A., Karniadakis, G.E., 2020. Hidden fluid mechanics: Learning velocity and pressure fields from flow visualizations. *Science* 367 (6481), 1026–1030. <http://dx.doi.org/10.1126/science.aaw4741>.
- Rotkopf, L.T., Ziener, C.H., von Knebel Doeberitz, N., Wolf, S.D., Hohmann, A., Wick, W., Bendszus, M., Schlemmer, H.-P., Paech, D., Kurz, F.T., 2024. A physics-informed deep learning framework for dynamic susceptibility contrast perfusion MRI. *Med. Phys.* 51 (12), 9031–9040. <http://dx.doi.org/10.1002/mp.17415>.
- Sadeghi, R., Gasner, N., Khodaei, S., Garcia, J., Keshavarz-Motamed, Z., 2022. Impact of mixed valvular disease on coarctation hemodynamics using patient-specific lumped parameter and lattice Boltzmann modeling. *Int. J. Mech. Sci.* 217, 107038. <http://dx.doi.org/10.1016/j.ijmecsci.2021.107038>.
- Samaniego, E., Anitescu, C., Goswami, S., Nguyen-Thanh, V., Guo, H., Hamdia, K., Zhuang, X., Rabczuk, T., 2020. An energy approach to the solution of partial differential equations in computational mechanics via machine learning: Concepts, implementation and applications. *Comput. Methods Appl. Mech. Engrg.* 362, 112790. <http://dx.doi.org/10.1016/j.cma.2019.112790>.
- Sarabian, M., Babaee, H., Laksari, K., 2022. Physics-informed neural networks for brain hemodynamic predictions using medical imaging. *IEEE Trans. Med. Imaging* 41 (9), 2285–2303. <http://dx.doi.org/10.1109/TMI.2022.3161653>.
- Sautory, T., Shadden, S.C., 2024. Unsupervised denoising and super-resolution of vascular flow data by physics-informed machine learning. *J. Biomech. Eng.* 146 (9), 091006. <http://dx.doi.org/10.1115/1.4065165>.
- Sel, K., Mohammadi, A., Pettigrew, R.I., Jafari, R., 2023. Physics-informed neural networks for modeling physiological time series for cuffless blood pressure estimation. *Npj Digit. Med.* 6 (1), 110. <http://dx.doi.org/10.1038/s41746-023-00853-4>.
- Sen, A., Ghajar-Rahimi, E., Aguirre, M., Navarro, L., Goergen, C.J., Avril, S., 2024. Physics-informed graph neural networks to solve 1-D equations of blood flow. *Comput. Methods Programs Biomed.* 257, 108427. <http://dx.doi.org/10.1016/j.cmpb.2024.108427>.
- Shi, J., Manjunatha, K., Behr, M., Vogt, F., Reese, S., 2024. A physics-informed deep learning framework for modeling of coronary in-stent restenosis. *Biomech. Model. Mechanobiol.* 23 (2), 615–629. <http://dx.doi.org/10.1007/s10237-023-01796-1>.
- Si, D., Wu, Y., Xiao, J., Qin, X., Guo, R., Liu, B., Ning, Z., Yin, J., Gao, P., Liu, Y., Yang, D., Cheng, K., Chen, T., Cheng, Z., Lin, X., Fang, Q., Herzka, D.A., Ding, H., 2023. Three-dimensional high-resolution dark-blood late gadolinium enhancement imaging for improved atrial scar evaluation. *Radiology* 307 (5), <http://dx.doi.org/10.1148/radiol.222032>.
- Sotero, R.C., Sanchez-Bornot, J.M., Shaharabi-Farahani, I., 2024. Parameter estimation in brain dynamics models from resting-state fMRI data using physics-informed neural networks. <http://dx.doi.org/10.1109/ICBEA62825.2024.00022>.
- Suriani, I., van Houtte, J., de Boer, E.C., van Knippenberg, L., Manzari, S., Mischi, M., Bouwman, R.A., 2022. Carotid Doppler ultrasound for non-invasive haemodynamic monitoring: A narrative review. *Physiol. Meas.* 43 (10), 10TR01. <http://dx.doi.org/10.1088/1361-6579/ac96cb>.
- Thodi, B.T., Ambadipudi, S.V.R., Jabari, S.E., 2024. Fourier neural operator for learning solutions to macroscopic traffic flow models: Application to the forward and inverse problems. *Transp. Res. Part C: Emerg. Technol.* 160, 104500. <http://dx.doi.org/10.1016/j.trc.2024.104500>.
- Ur Rehman, M.A., Ekici, O., Farooq, M.A., Butt, K., Ajao-Olarinoye, M., Wang, Z., Liu, H., 2025. Fluid-structure interaction analysis of pulsatile flow in arterial aneurysms with physics-informed neural networks and computational fluid dynamics. *Phys. Fluids* 37 (3), 031913. <http://dx.doi.org/10.1063/5.0259296>.
- van Herten, R.L., Chiribiri, A., Breeuwer, M., Veta, M., Scannell, C.M., 2022. Physics-informed neural networks for myocardial perfusion MRI quantification. *Med. Image Anal.* 78, 102399. <http://dx.doi.org/10.1016/j.media.2022.102399>.
- Voorter, P.H.M., Backes, W.H., Gurney-Champion, O.J., Wong, S.-M., Staals, J., van Oostenbrugge, R.J., van der Thiel, M.M., Jansen, J.F.A., Drenthen, G.S., 2023. Improving microstructural integrity, interstitial fluid, and blood microcirculation images from multi-b-value diffusion MRI using physics-informed neural networks in cerebrovascular disease. *Magn. Reson. Med.* 90 (4), 1657–1671. <http://dx.doi.org/10.1002/mrm.29753>.

- Voorter, P.H.M., Jansen, J.F.A., van der Thiel, M.M., van Dinther, M., Postma, A.A., van Oostenbrugge, R.J., Gurney-Champion, O.J., Drenthen, G.S., Backes, W.H., 2025. Diffusion-derived intravoxel-incoherent motion anisotropy relates to CSF and blood flow. *Magn. Reson. Med.* 93 (3), 930–941. <http://dx.doi.org/10.1002/mrm.30294>.
- Wang, L., Li, J., Chen, S., Fan, Z., Zeng, Z., Liu, Y., 2024. Finite difference-embedded UNet for solving transcranial ultrasound frequency-domain wavefield. *J. Acoust. Soc. Am.* 155 (3), 2257–2269. <http://dx.doi.org/10.1121/10.0025391>.
- Wang, H., Uhlmann, K., Vedula, V., Balzani, D., Varnik, F., 2022. Fluid-structure interaction simulation of tissue degradation and its effects on intra-aneurysm hemodynamics. *Biomech. Model. Mechanobiol.* 21 (2), 671–683. <http://dx.doi.org/10.1007/s10237-022-01556-7>.
- Wang, S., Wang, H., Perdikaris, P., 2021. Learning the solution operator of parametric partial differential equations with physics-informed DeepONets. *Sci. Adv.* 7 (40), eabi8605. <http://dx.doi.org/10.1126/sciadv.abi8605>.
- Wang, C., Zhao, W., Ruan, Z., Pu, Z., Wan, M., Fu, C., Wang, D., 2025. Enhanced physics-informed generative adversarial network to estimate spatial-temporal distribution of shear stress in carotid arteries. *Phys. Fluids* 37 (2), 021922. <http://dx.doi.org/10.1063/5.0252895>.
- Williams, K.A., Shields, A., Shiraz Bhurwani, M.M., Nagesh, S.V.S., Bednarek, D.R., Rudin, S., Ionita, C.N., 2023. Use of high-speed angiography HSA-derived boundary conditions and physics informed neural networks (PINNs) for comprehensive estimation of neurovascular hemodynamics. *Prog. Biomed. Opt. Imaging-Proc. SPIE* 12463, 124630Z. <http://dx.doi.org/10.1117/12.2654261>.
- Wong, H.S., Chan, W.X., Mao, W., Yap, C.H., 2025. 3D velocity and pressure field reconstruction in the cardiac left ventricle via physics informed neural network from echocardiography guided by 3D color Doppler. *Comput. Methods Programs Biomed.* 263, <http://dx.doi.org/10.1016/j.cmpb.2025.108671>.
- Wu, C., Zhu, M., Tan, Q., Kartha, Y., Liu, L., 2023. A comprehensive study of non-adaptive and residual-based adaptive sampling for physics-informed neural networks. *Comput. Methods Appl. Mech. Engrg.* 403, 115671. <http://dx.doi.org/10.1016/j.cma.2022.115671>.
- Yang, L., Meng, X., Karniadakis, G.E., 2021. B-PINNs: Bayesian physics-informed neural networks for forward and inverse PDE problems with noisy data. *J. Comput. Phys.* 425, 109913. <http://dx.doi.org/10.1016/j.jcp.2020.109913>.
- Yu, X.-L., Zhou, X.-P., 2023. A nonlocal energy-informed neural network for isotropic elastic solids with cracks under thermomechanical loads. *Internat. J. Numer. Methods Engrg.* 124 (18), 3935–3963. <http://dx.doi.org/10.1002/nme.7296>.
- Yu, X.-L., Zhou, X.-P., 2024a. A nonlocal energy-informed neural network based on peridynamics for elastic solids with discontinuities. *Comput. Mech.* 73 (2), 233–255. <http://dx.doi.org/10.1007/s00466-023-02365-0>.
- Yu, X.-L., Zhou, X.-P., 2024b. A nonlocal energy-informed neural network for peridynamic correspondence material models. *Eng. Anal. Bound. Elem.* 160, 273–297. <http://dx.doi.org/10.1016/j.enganabound.2024.01.004>.
- Yuan, L., Ni, Y.-Q., Deng, X.-Y., Hao, S., 2022. A-PINN: Auxiliary physics informed neural networks for forward and inverse problems of nonlinear integro-differential equations. *J. Comput. Phys.* 462, 111260. <http://dx.doi.org/10.1016/j.jcp.2022.111260>.
- Zafar, H., Ahmad, Liu, X., Sadiq, M.N., 2025. Optimizing physics-informed neural networks with hybrid activation functions: A comparative study on improving residual loss and accuracy using partial differential equations. *Chaos Solitons Fractals* 191, 115727. <http://dx.doi.org/10.1016/j.chaos.2024.115727>.
- Zhang, H., Chan, R.H., Tai, X.-C., 2024a. A meshless solver for blood flow simulations in elastic vessels using a physics-informed neural network. *SIAM J. Sci. Comput.* 46 (4), C479 – C507. <http://dx.doi.org/10.1137/23M1622696>.
- Zhang, D., Chen, Y., Chen, S., 2024b. Filtered partial differential equations: A robust surrogate constraint in physics-informed deep learning framework. *J. Fluid Mech.* 999, A40. <http://dx.doi.org/10.1017/jfm.2024.471>.
- Zhang, X., Mao, B., Che, Y., Kang, J., Luo, M., Qiao, A., Liu, Y., Anzai, H., Ohta, M., Guo, Y., Li, G., 2023. Physics-informed neural networks (PINNs) for 4D hemodynamics prediction: An investigation of optimal framework based on vascular morphology. *Comput. Biol. Med.* 164, 107287. <http://dx.doi.org/10.1016/j.combiommed.2023.107287>.
- Zhang, H., Tai, X.-C., 2024. Full 3D blood flow simulation in curved deformable vessels using physics-informed neural networks. *Acta Math. Univ. Comen.* 93 (4), 235–250.
- Zhou, X.-P., Yu, X.-L., 2024. Transfer learning enhanced nonlocal energy-informed neural network for quasi-static fracture in rock-like materials. *Comput. Methods Appl. Mech. Engrg.* 430, 117226. <http://dx.doi.org/10.1016/j.cma.2024.117226>.